PHYSICAL REVIEW D **92,** 115015 (2015)

Adjoint $SU(5)$ GUT model with T_7 flavor symmetry

Carolina Arbeláez,[*] A. E. Cárcamo Hernández,[†] Sergey Kovalenko,[‡] and Iván Schmidt[§]
Universidad Técnica Federico Santa María and Centro Científico-Tecnológico de Valparaíso, Casilla 110-V, Valparaíso, Chile
(Received 14 July 2015; published 18 December 2015)

We propose an adjoint $SU(5)$ GUT model with a T_7 family symmetry and an extra $Z_2 \otimes Z_3 \otimes Z_4 \otimes Z_4' \otimes Z_{12}$ discrete group that successfully describes the prevailing Standard Model fermion mass and mixing pattern. The observed hierarchy of the charged fermion masses and the quark mixing angles arises from the $Z_3 \otimes Z_4 \otimes Z_{12}$ symmetry breaking, which occurs near the GUT scale. The light active neutrino masses are generated by type-I and type-III seesaw mechanisms mediated by the fermionic $SU(5)$ singlet and the adjoint **24**-plet. The model predicts the effective Majorana neutrino mass parameter of neutrinoless double beta decay to be $m_{\beta\beta} = 4$ and 50 meV for the normal and the inverted neutrino spectra, respectively. We construct several benchmark scenarios, which lead to $SU(5)$ gauge coupling unification and are compatible with the known phenomenological constraints originating from the lightness of neutrinos, proton decay, dark matter, etc. These scenarios contain TeV-scale colored fields, which could give rise to a visible signal or be stringently constrained at the LHC.

DOI: 10.1103/PhysRevD.92.115015 PACS numbers: 12.60.Cn, 11.30.Hv, 12.15.Ff, 12.10.Dm

I. INTRODUCTION

The LHC discovery of a 126 GeV Higgs boson [1] has completed the era of the experimental quest for the missing elements of the Standard Model (SM). Now it is a well-established and extremely successful theory of the electroweak phenomena. However, the SM has several unaddressed issues, such as the smallness of neutrino masses, the observed pattern of fermion masses and mixings, and the existence of three fermion families [2], etc. The observed pattern of fermion masses spans a range of 5 orders of magnitude in the quark sector and much wider considering neutrinos. Neutrino oscillation experiments demonstrated that at least two of the neutrinos are massive, with masses much lower, by several orders of magnitude, than the other SM fermions, and also that all of the three neutrino flavors mix with each other. The smallness of quark mixing contrasts with the sizable mixing of neutrinos; i.e., while in the quark sector all the mixing angles are small, in the neutrino sector two of them are large, and only one mixing angle is small. This suggests that the neutrino sector is described by a different kind of underlying physics than the quark sector. As is well known, the tiny neutrino masses may point towards a high-energy scale of New Physics, where lepton-number violation (LNV) takes place.

The physical observables in the neutrino sector—i.e., the neutrino mass-squared splittings and mixing parameters—are constrained from the global fits of the available data from neutrino oscillation experiments by Daya Bay [3], T2K [4], MINOS [5], Double CHOOZ [6], and RENO [7], as shown in Tables I and II (based on Ref. [8]) for the normal (NH) and inverted (IH) hierarchies of the neutrino mass spectrum. As seen from these tables, the neutrino oscillation experimental data show a clear evidence of a violation of the so-called tribimaximal symmetry described by the tribimaximal mixing matrix (TBM), predicting the neutrino mixing angles $(\sin^2\theta_{12})_{\rm TBM}=\frac{1}{3}$, $(\sin^2\theta_{23})_{\rm TBM}=\frac{1}{2}$, and $(\sin^2\theta_{13})_{\rm TBM}=0$.

Addressing the flavor puzzle requires extensions of the SM, including larger scalar and/or fermion sectors, as well as an extended gauge group with additional flavor symmetries, which allow one to explain the SM fermion mass and mixing pattern. Along this line, several models have been proposed in the literature (for a review, see, e.g., Refs. [9–13]). The fermion mass and mixing pattern can also be described by postulating particular mass-matrix textures (see, e.g., Ref. [14] for a comprehensive review and some recent works considering textures). It is believed that grand unified theories (GUTs) endowed with flavor symmetries could provide an unified description for the mass and mixing pattern of leptons and quarks. This is motivated by the fact that leptons and quarks belong to the same multiplets of the GUT group, allowing one to relate their masses and mixings [15–17]. Furthermore, this setup can generate small neutrino masses through a type-I seesaw mechanism, where the new heavy Majorana neutrinos acquire very large masses due to their interactions with scalar singlets, assumed to get vacuum expectation values (VEVs) at the very high energy scale. Various GUT models with flavor symmetries have been proposed in the literature [18–37]. For a general review, see for example [38,39].

[*]carbela.arbelaez@usm.cl
[†]antonio.carcamo@usm.cl
[‡]sergey.kovalenko@usm.cl
[§]ivan.schmidt@usm.cl

TABLE I. Range for experimental values of neutrino mass-squared splittings and leptonic mixing parameters, taken from Ref. [8], for the case of normal hierarchy.

Parameter	$\Delta m^2_{21}(10^{-5}\ \mathrm{eV}^2)$	$\Delta m^2_{31}(10^{-3}\ \mathrm{eV}^2)$	$(\sin^2\theta_{12})_{\mathrm{exp}}$	$(\sin^2\theta_{23})_{\mathrm{exp}}$	$(\sin^2\theta_{13})_{\mathrm{exp}}$
Best fit	7.60	2.48	0.323	0.567	0.0234
1σ range	7.42–7.79	2.41–2.53	0.307–0.339	0.439–0.599	0.0214–0.0254
2σ range	7.26–7.99	2.35–2.59	0.292–0.357	0.413–0.623	0.0195–0.0274
3σ range	7.11–8.11	2.30–2.65	0.278–0.375	0.392–0.643	0.0183–0.0297

In this paper we propose a version of the adjoint $SU(5)$ GUT model where an extra $Z_2 \otimes Z_3 \otimes Z_4 \otimes Z_4' \otimes Z_{12}$ discrete group (see Ref [40] for a comprehensive study of the T_7 flavor group) extends the symmetry of the model, and several scalar fields are included to generate viable and predictive textures for the fermion sector. The particular role of each additional scalar field and the corresponding particle assignments under the symmetry group of the model are explained in detail in Sec. II. The fermionic sector of our model, in addition to the SM fermions, contains one heavy Majorana neutrino N_R, singlet under the SM group, and an adjoint **24** fermionic irreducible representation (irrep) of $SU(5)$ so that the light neutrino masses are generated via type-I and type-III seesaw mechanisms. An adjoint $SU(5)$ GUT model, but without discrete symmetries, and with more minimal particle content, was previously considered in Ref. [41]. Although our model is less minimal than that of Ref. [41], it provides a successful description of the SM fermion mass and mixing pattern, not addressed in Ref. [41]. Also, our model is more predictive in the leptonic sector.

The model has 14 free effective parameters, which allow us to reproduce the experimental values of 18 observables with good accuracy: i.e., 9 charged fermion masses, 2 neutrino mass-squared splittings, 3 lepton mixing parameters, and 4 parameters of the Wolfenstein CKM quark mixing matrix parametrization. It is noteworthy that the alternative $SU(5)$ GUT model of Ref. [25], with a supersymmetric setup and flavor symmetries, also has 14 free effective parameters aimed at reproducing the above mentioned 18 observables. Discrete symmetries different from T_7 have also been employed in adjoint $SU(5)$ GUT models. Some examples are the supersymmetric adjoint $SU(5)$ GUT model with A_4 flavor symmetry of Ref. [29], and the nonsupersymmetric $SU(5)$ GUT model with Z_4 symmetry of Ref. [30]. The aforementioned SUSY adjoint $SU(5)$ GUT model with A_4 flavor symmetry employs two sets of Z_2 symmetries and two sets of $U(1)$ symmetries. One of these $U(1)$ symmetries is global and represents an R-parity symmetry, whereas the other $U(1)$ symmetry is assumed to be gauged. The two Z_2 symmetries shape the Yukawa matrices for quarks and charged leptons. That model includes Higgs multiplets in **1**, **5**, $\bar{\mathbf{5}}$, $\overline{\mathbf{45}}$, dimensional representations of $SU(5)$. The 14 $SU(5)$ scalar singlets are grouped into three A_4 triplets and two A_4 trivial singlets. As in our model, neutrino masses arise from a combination of type-I and type-III seesaw mechanisms. Whereas in the model of Ref. [29], the CKM quark mixing matrix mainly arises from the down-type quark sector; in our model, the quark mixing is completely determined from the up-type quark sector. Furthermore, in this model the leptonic mixing angles are determined by two parameters, whereas in our model only one parameter determines the leptonic mixing angles. Moreover, the quark masses and mixings are studied in detail in our model, whereas in the model of Ref. [29] a detailed study of quark masses and mixings is not included. Besides that, our model includes a detailed discussion of gauge coupling unification and seesaw mass scale limits, not performed in the model of Ref. [29]. With respect to the nonsupersymmetric adjoint $SU(5)$ GUT model with Z_4 discrete symmetry of Ref. [30], the discrete symmetry is introduced in that model in order to generate the nearest-neighbor-interaction textures for charged fermions. The scalar sector of that model includes an adjoint multiplet, a quintuplet and one **45**-dimensional representation, and neutrino masses arise from type-I seesaw,

TABLE II. Range for experimental values of neutrino mass-squared splittings and leptonic mixing parameters, taken from Ref. [8], for the case of inverted hierarchy.

Parameter	$\Delta m^2_{21}(10^{-5}\ \mathrm{eV}^2)$	$\Delta m^2_{13}(10^{-3}\ \mathrm{eV}^2)$	$(\sin^2\theta_{12})_{\mathrm{exp}}$	$(\sin^2\theta_{23})_{\mathrm{exp}}$	$(\sin^2\theta_{13})_{\mathrm{exp}}$
Best fit	7.60	2.38	0.323	0.573	0.0240
1σ range	7.42–7.79	2.32–2.43	0.307–0.339	0.530–0.598	0.0221–0.0259
2σ range	7.26–7.99	2.26–2.48	0.292–0.357	0.432–0.621	0.0202–0.0278
3σ range	7.11–8.11	2.20–2.54	0.278–0.375	0.403–0.640	0.0183–0.0297

type-III seesaw, and one-loop radiative seesaw mechanisms. Despite the fact that this model is more minimal than our T_7 flavor adjoint $SU(5)$ GUT model, our model has a much more predictive lepton sector. Let us note that the lepton sector of the model of Ref. [30] has 12 effective free parameters, whereas the lepton sector of our model has a total of 6 effective free parameters. Unlike the models of Refs. [29,30], our adjoint $SU(5)$ GUT model, which is nonsupersymmetric, employs a $Z_2 \otimes Z_3 \otimes Z_4 \otimes Z_4' \otimes Z_{12}$ discrete symmetry.

After imposing gauge coupling unification equal to or better than that in the MSSM (another difference with respect to Refs. [41,42], which impose exact gauge coupling unification), we find a wide set of simple field configurations, which pass proton decay constraints and give rise to the neutrino masses through a type-I and type-III seesaw realization. Considering the limit on the triplet scalar mass (denoted here as Ξ_3), which comes from the cold dark matter constraints pointed out in Ref. [43], we found lower limits on the seesaw scale for two simple scenarios with different sets of beyond-the-SM field configurations.

The paper is organized as follows: In Sec. II we outline the proposed model. In Sec. III we present our results on neutrino masses and mixing, followed by a numerical analysis. Our results for the quark sector, with the corresponding numerical analysis, are presented in Sec. IV. Gauge coupling unification and seesaw scale mass limits are discussed in Sec V. We conclude with discussions and a summary in Sec. VI. Some necessary facts about the T_7 group and details of our analysis are collected in appendixes.

II. THE MODEL

The first grand unified theory (GUT) proposed in Ref. [44] is based on the $SU(5)$ gauge symmetry accommodating the SM fermions in $\bar{\mathbf{5}} + \mathbf{10}$ and the scalars in $\mathbf{5} + \mathbf{24}$ irreps of $SU(5)$. As is well known, this model suffers from several problems. In particular, it predicts wrong down-type quark and charged lepton mass relations and a short proton lifetime, and the unification of gauge couplings disagrees with the values of α_S, $\sin\theta_W$, and α_{em} measured at the M_Z scale. Moreover, this minimal $SU(5)$ GUT model does not include a mechanism for generating nonvanishing neutrino masses in contradiction with experimental data on neutrino oscillations. The minimal $SU(5)$ GUT model can be improved by including, in particular, a scalar $\mathbf{45}$ irrep of $SU(5)$ [42,43,45–55]. This next-to-minimal $SU(5)$ GUT model fails, however, in describing the observed pattern of fermion masses and mixings, due to the lack of explanation for the hierarchy among the large number of Yukawa couplings in the model. Below we consider a multi-Higgs extension of the next-to-minimal $SU(5)$ GUT model, which successfully describes the pattern of the SM fermion masses and mixing. The full symmetry $\mathcal{G}$ of the model is broken in two subsequent steps as follows:

$$\begin{aligned}\mathcal{G} &= SU(5) \otimes T_7 \otimes Z_2 \otimes Z_3 \otimes Z_4 \otimes Z_4' \otimes Z_{12} \\ &\Downarrow \Lambda_{\rm GUT} \\ &SU(3)_C \otimes SU(2)_L \otimes U(1)_Y \\ &\Downarrow \Lambda_{\rm EW} \\ &SU(3)_C \otimes U(1)_{em}. \end{aligned} \tag{1}$$

Let us note that among the discrete symmetries we introduced the non-Abelian flavor symmetry group T_7, which is the smallest group with a complex triplet representation, allowing us to naturally accommodate the three families of fermions.

The fermion assignments under the group $\mathcal{G} = SU(5) \otimes T_7 \otimes Z_2 \otimes Z_3 \otimes Z_4 \otimes Z_4' \otimes Z_{12}$ are

$$\begin{aligned}
&\Psi_{ij}^{(1)} \sim (\mathbf{10}, \mathbf{1_0}, 1, \omega, 1, 1, i), \\
&\Psi_{ij}^{(2)} \sim (\mathbf{10}, \mathbf{1_1}, 1, \omega^2, 1, 1, e^{\frac{\pi i}{3}}), \\
&\Psi_{ij}^{(3)} \sim (\mathbf{10}, \mathbf{1_2}, 1, 1, 1, 1, 1), \qquad i,j = 1,2,3,4,5, \\
&\psi^i = (\psi^{i(1)}, \psi^{i(2)}, \psi^{i(3)}) \sim (\bar{\mathbf{5}}, \bar{\mathbf{3}}, 1, 1, 1, 1, 1), \\
&N_R \sim (\mathbf{1}, \mathbf{1_0}, -1, 1, 1, -1, -1), \\
&\rho \sim (\mathbf{24}, \mathbf{1_0}, -1, 1, 1, -i, 1),
\end{aligned} \tag{2}$$

where $\omega = e^{\frac{2\pi i}{3}}$.

More explicitly, the fermions are accommodated as

$$\Psi_{ij}^{(f)} = \frac{1}{\sqrt{2}} \begin{pmatrix} 0 & u_3^{(f)c} & -u_2^{(f)c} & -u_1^{(f)} & -d_1^{(f)} \\ -u_3^{(f)c} & 0 & u_1^{(f)c} & -u_2^{(f)} & -d_2^{(f)} \\ u_2^{(f)c} & -u_1^{(f)c} & 0 & -u_3^{(f)} & -d_3^{(f)} \\ u_1^{(f)} & u_2^{(f)} & u_3^{(f)} & 0 & -l^{(f)c} \\ d_1^{(f)} & d_2^{(f)} & d_3^{(f)} & l^{(f)c} & 0 \end{pmatrix}_L, \tag{3}$$

$$f = 1,2,3, \qquad i,j = 1,2,3,4,5,$$

$$\psi^{i(f)} = (d_1^{(f)c}, d_2^{(f)c}, d_3^{(f)c}, l^{(f)}, -\nu_f)_L. \tag{4}$$

Here the subscripts correspond to the different quark colors, while the superscript f refers to fermion families. One can see that the three families of left- and right-handed fermions, corresponding to the $\bar{\mathbf{5}}$ irrep of $SU(5)$, are unified into a T_7 antitriplet $\bar{\mathbf{3}}$, while the three families of left- and right-handed fermions corresponding to the $\mathbf{10}$ irreps of $SU(5)$ are assigned to the three different T_7 singlets $\mathbf{1_0}$, $\mathbf{1_1}$, $\mathbf{1_2}$.

The scalar sector is composed of the following $SU(5)$ representations: one $\mathbf{24}$, one $\mathbf{45}$, four $\mathbf{5}$'s and ten

1's. Two sets of $SU(5)$ singlets are unified into two T_7 triplets. The remaining scalar fields, i.e., one **45**, one **24**, four **5**'s and the remaining four **1**'s, are accommodated by three T_7 singlets. Thus, the $\mathcal{G}$ assignments of the scalar fields are

$$\begin{aligned}
\sigma &\sim (\mathbf{1},\mathbf{1_0},1,1,1,1,e^{-\frac{i\pi}{6}}),\\
\tau &\sim (\mathbf{1},\mathbf{1_0},1,\omega,i,1,e^{-\frac{i\pi}{6}}),\\
\xi = (\xi_1,\xi_2,\xi_3) &\sim (\mathbf{1},\mathbf{3},-1,1,1,1,1),\\
\varphi &\sim (\mathbf{1},\mathbf{1_0},1,\omega,-1,1,1),\\
\eta &\sim (\mathbf{1},\mathbf{1},1,1,1,-1,1),\\
\chi = (\chi_1,\chi_2,\chi_3) &\sim (\mathbf{1},\mathbf{3},1,1,1,i,e^{\frac{i\pi}{3}}),\\
H_i^{(1)} &\sim (\mathbf{5},\mathbf{1_0},-1,1,1,1,e^{-\frac{i\pi}{3}}),\\
H_i^{(2)} &\sim (\mathbf{5},\mathbf{1_0},1,\omega,1,1,1),\\
H_i^{(3)} &\sim (\mathbf{5},\mathbf{1_1},1,\omega^2,1,1,1),\\
H_i^{(4)} &\sim (\mathbf{5},\mathbf{1_2},1,1,1,1,1),\\
\Xi_j^i &\sim (\mathbf{24},\mathbf{1_0},1,1,1,1,1),\\
\Phi_{jk}^i &\sim (\mathbf{45},\mathbf{1_0},-1,1,1,1,e^{-\frac{i\pi}{3}}).
\end{aligned} \tag{5}$$

The VEVs of the scalars $H_i^{(h)}$ $(h=1,2,3,4)$ and Ξ_j^i are

$$\begin{aligned}
\langle H_i^{(h)}\rangle &= v_H^{(h)}\delta_{i5}, \qquad h=1,2,3,4,\\
\langle \Xi_j^i\rangle &= \frac{2v_\Xi}{\sqrt{30}}\mathrm{diag}\left(1,1,1,-\frac{3}{2},-\frac{3}{2}\right),\\
i,j &= 1,2,3,4,5.
\end{aligned} \tag{6}$$

Note that the VEV pattern for the Ξ field given above is consistent with the minimization conditions of the model scalar potential and follows from the general group theory analysis of spontaneous symmetry breakdown [56].

The following comments about the possible VEV patterns for the T_7 scalar triplets χ and ξ are in order. Here we assume a hierarchy between the VEVs of the T_7 scalar triplets χ and ξ, i.e., $v_\chi \ll v_\xi$, which implies that the mixing angle between the the T_7 scalar triplets χ and ξ is strongly suppressed, since it is of the order of $\frac{v_\chi}{v_\xi}$, as follows from the method of recursive expansion of Refs. [57–59]. Consequently, the mixing between the T_7 scalar triplets χ and ξ can be neglected. The parts of the scalar potential for each of the two T_7 scalar triplets at the renormalizable level are given by

$$\begin{aligned}
V_{T7}^{(1)} = &-\mu_\chi^2(\chi\chi^*)_{\mathbf{1_0}} + \kappa_{\chi,1}(\chi\chi^*)_{\mathbf{3}}(\chi\chi^*)_{\bar{\mathbf{3}}} + \kappa_{\chi,2}(\chi\chi)_{\mathbf{3}}(\chi^*\chi^*)_{\bar{\mathbf{3}}} + \kappa_{\chi,3}(\chi\chi)_{\bar{\mathbf{3}}}(\chi^*\chi^*)_{\mathbf{3}}\\
&+ \kappa_{\chi,4}(\chi\chi^*)_{\mathbf{1_0}}(\chi\chi^*)_{\mathbf{1_0}} + \kappa_{\chi,5}(\chi\chi^*)_{\mathbf{1_1}}(\chi\chi^*)_{\mathbf{1_2}} + \mathrm{H.c.},
\end{aligned} \tag{7}$$

$$\begin{aligned}
V_{T7}^{(2)} = &-\mu_\xi^2(\xi\xi^*)_{\mathbf{1_0}} + \kappa_{\xi,1}(\xi\xi^*)_{\mathbf{3}}(\xi\xi^*)_{\bar{\mathbf{3}}} + \kappa_{\xi,2}(\xi\xi)_{\mathbf{3}}(\xi^*\xi^*)_{\bar{\mathbf{3}}} + \kappa_{\xi,3}(\xi^*\xi^*)_{\mathbf{3}}(\xi\xi)_{\bar{\mathbf{3}}}\\
&+ \kappa_{\xi,4}(\xi\xi^*)_{\mathbf{1_0}}(\xi\xi^*)_{\mathbf{1_0}} + \kappa_{\xi,5}(\xi\xi^*)_{\mathbf{1_1}}(\xi\xi^*)_{\mathbf{1_2}} + \mathrm{H.c.}
\end{aligned} \tag{8}$$

In the part of the scalar potential for each T_7 scalar triplet there are six free parameters: one bilinear and five quartic couplings. The minimization conditions of $V_{T7}^{(1)}$ and $V_{T7}^{(2)}$ lead to the following relations:

$$\begin{aligned}
\frac{\partial\langle V_{T7}^{(m)}\rangle}{\partial v_{S_1}} &= -2v_{S_1}\mu_S + 4\kappa_{S,1}v_{S_1}(v_{S_2}^2+v_{S_3}^2) + 4(\kappa_{S,2}+\kappa_{S,3})[3v_{S_1}^2v_{S_3}\cos(\theta_{S_1}-\theta_{S_3}) + v_{S_2}^3\cos(\theta_{S_1}-\theta_{S_2})]\\
&\quad + 8\kappa_{S,4}v_{S_1}(v_{S_1}^2+v_{S_2}^2+v_{S_3}^2) + 4\kappa_{S,5}v_{S_1}(2v_{S_1}^2-v_{S_2}^2-v_{S_3}^2)\\
&= 0,\\
\frac{\partial\langle V_{T7}^{(m)}\rangle}{\partial v_{S_2}} &= -2v_{S_2}\mu_S + 4\kappa_{S,1}v_{S_2}(v_{S_1}^2+v_{S_3}^2) + 4(\kappa_{S,2}+\kappa_{S,3})[3v_{S_2}^2v_{S_1}\cos(\theta_{S_1}-\theta_{S_2}) + v_{S_3}^3\cos(\theta_{S_2}-\theta_{S_3})]\\
&\quad + 8\kappa_{S,4}v_{S_2}(v_{S_1}^2+v_{S_2}^2+v_{S_3}^2) + 4\kappa_{S,5}v_{S_2}(2v_{S_2}^2-v_{S_1}^2-v_{S_3}^2)\\
&= 0,\\
\frac{\partial\langle V_{T7}^{(m)}\rangle}{\partial v_{S_3}} &= -2v_{S_3}\mu_S + 4\kappa_{S,1}v_{S_3}(v_{S_1}^2+v_{S_2}^2) + 4(\kappa_{S,2}+\kappa_{S,3})[3v_{S_3}^2v_{S_2}\cos(\theta_{S_2}-\theta_{S_3}) + v_{S_1}^3\cos(\theta_{S_1}-\theta_{S_3})]\\
&\quad + 8\kappa_{S,4}v_{S_3}(v_{S_1}^2+v_{S_2}^2+v_{S_3}^2) + 4\kappa_{S,5}v_{S_3}(2v_{S_3}^2-v_{S_1}^2-v_{S_2}^2)\\
&= 0,
\end{aligned} \tag{9}$$

where $m = 1, 2$, $S = \chi, \xi$ and $\langle S \rangle = (v_{S_1} e^{i\theta_{S_1}}, v_{S_2} e^{i\theta_{S_2}}, v_{S_3} e^{i\theta_{S_3}})$. Then, from an analysis of the minimization equations given by Eq. (9) and setting $\kappa_{\chi,2} = -\kappa_{\chi,3}$, we obtain for a large range of the parameter space the following VEV direction:

$$v_{\chi_1} = e^{-\frac{i\phi}{2}} \frac{v_\chi}{\sqrt{2}}, \qquad v_{\chi_3} = e^{\frac{i\phi}{2}} \frac{v_\chi}{\sqrt{2}}, \qquad v_{\chi_2} = 0,$$
$$v_{\xi_1} = v_{\xi_2} = v_{\xi_3} = \frac{v_\xi}{\sqrt{3}}. \tag{10}$$

In the case of ξ, this is a vacuum configuration preserving a Z_3 subgroup of T_7, which has been extensively studied by many authors (see, for example, Ref. [40]). The VEV pattern for χ is similar to the one we previously studied in an $SU(5)$ model and in a 6HDM with A_4 flavor symmetry [34,60]. It is worth mentioning that there could be relative phases between the different components of $\langle \xi \rangle$, consistent with the scalar potential minimization equations, as follows from the expressions given in Eq. (9). We have checked that the nonvanishing phases consistent with the scalar potential minimization equations satisfy $\theta_{S_i} = -\theta_{S_j} \neq \theta_{S_k}$, with $i \neq j \neq k$ $(i, j, k = 1, 2, 3)$. Moreover, we checked that the physical observables in the lepton sector, studied in Sec. III, do not depend on these phases. For generality we included nonzero phases in the $\langle \chi \rangle$ sector, as indicated in Eq. (10).

From the expressions given in Eq. (9), and using the vacuum configuration for the T_7 scalar triplets given in Eq. (10), we find the relation between the parameters and the magnitude of the VEV:

$$\mu_\chi^2 = (\kappa_{\chi,1} + 4\kappa_{\chi,4} + \kappa_{\chi,5}) v_\chi^2,$$
$$\mu_\xi^2 = \frac{4}{3}[\kappa_{\xi,1} + 2(\kappa_{\xi,2} + \kappa_{\xi,3}) + 3\kappa_{\xi,4}] v_\xi^2. \tag{11}$$

These results show that the VEV directions for the T_7 triplets χ and ξ in Eq. (10) are consistent with a global minimum of the scalar potential of our model.

Assuming that the charged fermion mass pattern and quark mixing hierarchy is caused by the Z_3, Z_4, and Z_{12} symmetries, and in order to relate the quark masses with the quark mixing parameters, we set the VEVs of the $SU(5)$ scalar singlets as follows:

$$v_\chi \ll v_\eta \sim v_\varphi = v_\tau = v_\xi = v_\sigma = \Lambda_{\rm GUT} = \lambda \Lambda, \tag{12}$$

where $\lambda = 0.225$ is one of the parameters in the Wolfenstein parametrization and Λ is the high-energy scale cutoff of our model, to be clarified below. Assuming that the parameters of the scalar interaction terms involving these $SU(5)$ scalar singlets are of the same order of magnitude, it is straightforward to show that the VEVs in Eq. (12) are consistent with the minimization conditions of the model scalar potential.

The fields Φ^i_{jk}, being the **45** irrep of $SU(5)$, satisfy the following relations:

$$\Phi^i_{jk} = -\Phi^i_{kj}, \quad \sum_{i=1}^{5} \Phi^i_{ij} = 0, \quad i, j, k = 1, 2, \ldots, 5. \tag{13}$$

Consequently, the only allowed nonzero VEVs of Φ^i_{jk} are

$$\langle \Phi^p_{p5} \rangle = -\frac{1}{3} \langle \Phi^4_{45} \rangle = v_\Phi,$$
$$\langle \Phi^i_{j5} \rangle = v_\Phi (\delta^i_j - 4\delta^i_4 \delta^4_j),$$
$$i, j = 1, 2, 3, 4, 5, \qquad p = 1, 2, 3, 5. \tag{14}$$

With the specified particle content, there are the following interaction terms, invariant under the group $\mathcal{G}$ and relevant for further analysis:

$$\begin{aligned}
\mathcal{L}_Y = {} & \alpha_1 (\psi^i \xi)_{\mathbf{1}_0} H^{j(1)} \Psi^{(1)}_{ij} \frac{\sigma^5 \varphi^2 + \kappa \sigma \tau^4 \varphi^{*2}}{\Lambda^8} + \alpha_2 (\psi^i \xi)_{\mathbf{1}_2} H^{j(1)} \Psi^{(2)}_{ij} \frac{\tau^4}{\Lambda^5} + \alpha_3 (\psi^i \xi)_{\mathbf{1}_1} H^{j(1)} \Psi^{(3)}_{ij} \frac{\sigma^2}{\Lambda^3} \\
& + \beta_1 (\psi^i \xi)_{\mathbf{1}_0} \Phi^{jk}_i \Psi^{(1)}_{jk} \frac{\sigma^5 \varphi^2 + \kappa \sigma \tau^4 \varphi^{*2}}{\Lambda^8} + \beta_2 (\psi^i \xi)_{\mathbf{1}_2} \Phi^{jk}_i \Psi^{(2)}_{jk} \frac{\tau^4}{\Lambda^5} + \beta_3 (\psi^i \xi)_{\mathbf{1}_1} \Phi^{jk}_i \Psi^{(3)}_{jk} \frac{\sigma^2}{\Lambda^3} \\
& + \varepsilon^{ijklp} \Big\{ \gamma_{11} \Psi^{(1)}_{ij} H^{(2)}_p \Psi^{(1)}_{kl} \frac{\sigma^6}{\Lambda^6} + \gamma_{12} \Psi^{(1)}_{ij} H^{(4)}_p \Psi^{(2)}_{kl} \frac{\sigma^5}{\Lambda^5} + \gamma_{21} \Psi^{(2)}_{ij} H^{(4)}_p \Psi^{(1)}_{kl} \frac{\sigma^5}{\Lambda^5} \\
& + \gamma_{22} \Psi^{(2)}_{ij} H^{(3)}_p \Psi^{(2)}_{kl} \frac{\sigma^4}{\Lambda^4} + \gamma_{13} \Psi^{(1)}_{ij} H^{(3)}_p \Psi^{(3)}_{kl} \frac{\sigma^3}{\Lambda^3} + \gamma_{31} \Psi^{(3)}_{ij} H^{(3)}_p \Psi^{(1)}_{kl} \frac{\sigma^3}{\Lambda^3} \\
& + \gamma_{23} \Psi^{(2)}_{ij} H^{(2)}_p \Psi^{(3)}_{kl} \frac{\sigma^2}{\Lambda^2} + \gamma_{32} \Psi^{(3)}_{ij} H^{(2)}_p \Psi^{(2)}_{kl} \frac{\sigma^2}{\Lambda^2} + \gamma_{33} \Psi^{(3)}_{ij} H^{(4)}_p \Psi^{(3)}_{kl} \Big\} \\
& + \frac{\lambda_{1\nu}}{\Lambda^2} [\psi^i (\chi^* \chi^*)_{\mathbf{3}}]_{\mathbf{1}_0} H^{(1)}_i N_R + \frac{\lambda_{2\nu}}{\Lambda^2} [(\psi^i \chi^*)_{\mathbf{3}} \chi^*]_{\mathbf{1}_0} H^{(1)}_i N_R + \frac{\lambda_{3\nu}}{\Lambda} (\psi^i \chi)_{\mathbf{1}_0} H^{(1)}_j \rho^j_i \\
& + \frac{\lambda_{4\nu}}{\Lambda} (\psi^i \chi)_{\mathbf{1}_0} \Phi^k_{ij} \rho^j_k + m_N \bar{N}_R N^c_R + y_1 \bar{N}_R N^c_R \frac{\sigma^* \sigma + x_1 \tau^* \tau + x_2 \varphi^* \varphi}{\Lambda} + y_2 Tr(\rho^2) \eta + y_3 Tr(\rho^2 \Xi) \frac{\eta}{\Lambda},
\end{aligned} \tag{15}$$

where the dimensionless couplings in Eq. (15) are $\mathcal{O}(1)$ parameters, and are assumed to be real, excepting γ_{11}, γ_{12}, γ_{21}, γ_{31} and γ_{13}, which are assumed to be complex. The subscripts $\mathbf{1_0}$, $\mathbf{1_1}$, $\mathbf{1_2}$ denote projecting out the corresponding T_7 singlet in the product of the two triplets. Let us note that Eq. (15) is $SU(5)$ invariant, since the scalar fields $H_p^{(h)}$, $H^{(h)p}$ $(h=1,2,3,4)$, Φ^i_{jk}, Φ_i^{jk} transform as $\mathbf{5}$, $\bar{\mathbf{5}}$, $\mathbf{45}$ and $\overline{\mathbf{45}}$ under $SU(5)$, respectively, and the fermionic fields ψ^i and $\Psi^{(f)}_{ij}$ $(f=1,2,3)$ as $\bar{\mathbf{5}}$ and $\mathbf{10}$, under the $SU(5)$ group, respectively. Besides that, it is worth mentioning that the scalar field $H^{(h)p}$ $(h=1,2,3,4)$ transforms with the opposite Z_N charges as compared to $H_p^{(h)}$. Furthermore, it is noteworthy that the term $Tr(\rho^2)$ is not present in Eq. (15), since this term is not invariant under the Z_4' symmetry. The lightest of the physical neutral scalar states of $H^{(1)}$, $H^{(2)}$, $H^{(3)}$, $H^{(4)}$ and Φ should be interpreted as the SM-like 126 GeV Higgs observed at the LHC.

Let us summarize and comment on the above presented model setup. In comparison with the next-to-minimal $SU(5)$ GUT model of Refs. [42,43,45–55], besides for the introduction of additional discrete symmetries, we also extended the fermionic sector by introducing one heavy Majorana neutrino N_R singlet under the SM group and a $\mathbf{24}$ fermionic irrep of $SU(5)$, namely ρ^i_j. We will show that since the Z_2 symmetry present in (1) is not preserved at low energies, the active neutrinos get tree-level masses via type-I and type-III seesaw mechanisms. In the next section, we will also show that in order to successfully accommodate the experimental data on neutrino mass-squared splittings, one needs both the SM singlet right-handed Majorana neutrino and the $\mathbf{24}$ fermionic irrep of $SU(5)$. Having only one of them would lead to two massless active neutrinos, in contradiction to the experimental data on neutrino oscillations. Note that our fermionic sector is less minimal than the one considered in Ref. [41] with only a $\mathbf{24}$ fermionic irrep of $SU(5)$. However, our model provides a successful description of the SM charged fermion masses and mixing pattern, not addressed in Ref. [41].

Despite the flavor-discrete groups in Eq. (1), the corresponding field assignment as well as the VEV pattern look rather sophisticated, although each introduced element plays its own role in the arrangement of the desired particle spectrum and flavor mixing. Let as briefly sketch our justification of the model setup:

(1) The scalar sector includes the following $SU(5)$ representations: one $\mathbf{24}$, one $\mathbf{45}$, four $\mathbf{5}$'s and ten $\mathbf{1}$'s. The $\mathbf{45}$ and the four $\mathbf{5}$'s scalar irreps of $SU(5)$ acquire VEVs at the electroweak scale, thus inducing the second step of symmetry breaking. The remaining scalars acquire VEVs at the GUT scale and trigger the first step of symmetry breaking. As previously mentioned, having scalar fields in the $\mathbf{45}$ representation of $SU(5)$ is crucial to get the correct mass relations of down-type quarks and charged leptons.

(2) The T_7 discrete group is crucial to generating textures for the lepton sector that successfully account for the experimentally observed deviation from the trimaximal mixing pattern that attracted a lot of attention in the literature as a framework for describing the lepton mixings; see for example Ref. [40]. To reproduce the nontrivial quark mixing consistent with experimental data, the up-type quark sector requires three $\mathbf{5}$'s, i.e., $H_i^{(2)}$, $H_i^{(3)}$, and $H_i^{(4)}$ irreps of $SU(5)$ assigned to different T_7 singlets. In the down-type quark sector, on the other hand, only one $\mathbf{5}$ irrep $H_i^{(1)}$, one $\mathbf{45}$ irrep Φ^i_{jk} assigned to T_7 trivial singlets and three $\mathbf{1}$'s, unified in the T_7 triplet ξ, are needed.

(3) The Z_2 symmetry separates the scalars in the $\mathbf{5}$ and $\mathbf{45}$ irreps of $SU(5)$ participating in the Yukawa interactions for charged leptons and down-type quarks from those ones participating in the Yukawa interactions for up-type quarks. This implies that the $SU(5)$ scalar multiplets contributing to the masses of the down-type quarks and charged leptons are different from those that provide masses to the up-type quarks. Furthermore, the Z_2 symmetry separates the T_7 scalar triplet ξ participating in the Yukawa interactions for charged leptons and down-type quarks from the one (χ) participating in the neutrino Yukawa interactions. In the scalar sector, the Z_2 symmetry distinguishes the T_7 scalar triplet ξ and the $SU(5)$ multiplets $H_i^{(1)}$ and Φ^i_{jk} charged under this symmetry from the remaining scalar fields, neutral under this symmetry. Because of this, the $\mathbf{45}$ and one of the 5s' scalars participate in the Yukawa interactions for leptons and down-type quarks, whereas the remaining $SU(5)$ multiplets participate in the Yukawa interactions for up-type quarks. This results in a reduction of parameters in the quark sector, since due to the Z_2 symmetry the $\mathbf{45}$ scalar irrep of $SU(5)$ does not appear in the up-type quark Yukawa terms. Furthermore, all fermions are Z_2 even, excepting the right-handed Majorana neutrino and the $\mathbf{24}$ fermionic irrep of $SU(5)$, which are Z_2 odd.

(4) As with the T_7 symmetry, the Z_4' symmetry is also necessary to get a predictive neutrino mass-matrix texture that only depends on three effective parameters and that gives rise to the experimentally observed deviation from the trimaximal mixing pattern. This symmetry also separates the $\mathbf{24}$ fermionic irrep ρ and the charged under this symmetry from the remaining fermionic fields, neutral under this symmetry.

(5) The Z_3 and Z_4 symmetries are crucial to getting the right pattern of charged lepton and down-type quark masses. The Z_3 symmetry distinguishes the three **10**'s irreps of $SU(5)$, having different Z_3 charges. The Z_4 symmetry separates the $SU(5)$ scalar singlets φ and τ, charged under this symmetry, from the remaining scalar fields, neutral under this symmetry. All the fermionic fields are assumed to transform trivially under the Z_4 symmetry. Without the Z_3 and Z_4 symmetries, the down-quark and electron masses would be larger by about 2 orders of magnitude than their corresponding experimental values, unless one sets the corresponding Yukawa couplings unnaturally small. It is noteworthy that, unlike in the up-type quark sector, a λ^8 suppression ($\lambda = 0.225$ is one of the Wolfenstein parameters) in the 11 entry of the mass matrices for down-type quarks and charged leptons is required to naturally explain the smallness of the down-quark and electron masses. The Z_3, Z_4, and Z_{12} symmetries will be crucial to achieve that λ^8 suppression.

(6) The Z_{12} symmetry shapes the hierarchical structure of the quark mass matrices necessary to get a realistic pattern of quark masses and mixings. Besides that, the charged lepton mass hierarchy also arises from the Z_{12} symmetry. Let us recall that due to the properties of the Z_N groups, it follows that Z_{12} is the lowest cyclic symmetry that allows building the dimension-ten up-type quark Yukawa term with a σ^6/Λ^6 insertion in a term of dimension four, crucial to getting the required λ^6 suppression in the 11 entry of the up-type quark mass matrix.

III. LEPTON MASSES AND MIXING

The charged lepton mass matrix is derived from Eq. (15) by using the product rules for the T_7 group given in Appendix A, and considering that the VEV pattern of the $SU(5)$ singlet T_7 scalar triplet ξ satisfies Eq. (10) with the VEVs of their components set to be equal to $\lambda\Lambda$ (Λ being the cutoff of our model), as indicated by Eq. (12). Then, the mass matrix for charged leptons takes the form

$$M_l = \frac{v}{\sqrt{2}} V_{lL}^{\dagger} \begin{pmatrix} a_1^{(l)}\lambda^8 & 0 & 0 \\ 0 & a_2^{(l)}\lambda^5 & 0 \\ 0 & 0 & a_3^{(l)}\lambda^3 \end{pmatrix} = V_{lL}^{\dagger}\,\mathrm{diag}(m_e, m_\mu, m_\tau), \tag{16}$$

with

$$a_1^{(l)} = \frac{1}{v}(\alpha_1 v_H^{(1)} - 6\beta_1 v_\Phi),$$
$$a_2^{(l)} = \frac{1}{v}(\alpha_2 v_H^{(1)} - 6\beta_2 v_\Phi),$$
$$a_3^{(l)} = \frac{1}{v}(\alpha_3 v_H^{(1)} - 6\beta_3 v_\Phi), \tag{17}$$

$$V_{lL} = \frac{1}{\sqrt{3}} \begin{pmatrix} 1 & 1 & 1 \\ 1 & \omega & \omega^2 \\ 1 & \omega^2 & \omega \end{pmatrix}, \qquad \omega = e^{\frac{2\pi i}{3}}. \tag{18}$$

Here $\lambda = 0.225$ is the Wolfenstein parameter. As was commented in the previous section, we assume that the dimensionless couplings α_i and β_i ($i = 1, 2, 3$) in Eq. (15) are roughly of the same order of magnitude and the VEVs $v_H^{(1)}$ and v_Φ are of the order of the electroweak scale $v \simeq 246$ GeV. Therefore, the hierarchy among the charged lepton masses arises from the breaking of the Z_3, Z_4 and Z_{12} symmetries. As seen, the lepton mass matrix Eq. (16) is fully determined in our model by three effective parameters $\alpha_{1,2,3}^{(l)}$ shown in Eq. (17), which we fit to reproduce the experimentally measured values of lepton masses and mixings at the M_Z scale. A similar situation takes place in the sector of quarks, as will be shown in the next section.

From the neutrino Yukawa terms of Eq. (15), and taking into account that the VEVs of the $SU(5)$ singlets φ, σ and τ are set to be equal to $\lambda\Lambda$ (where Λ is our model cutoff), as indicated by Eq. (12), we find that the fields contained in the **24** fermionic irrep of $SU(5)$ acquire very large masses, which are given by

$$m_{\rho_0} = y_2 v_\eta - \frac{y_3 v_\Xi v_\eta}{\sqrt{30}\Lambda},$$
$$m_{\rho_3} = y_2 v_\eta - \frac{3y_3 v_\Xi v_\eta}{\sqrt{30}\Lambda},$$
$$m_{\rho_8} = y_2 v_\eta + \frac{2y_3 v_\Xi v_\eta}{\sqrt{30}\Lambda},$$
$$m_{\rho_{(3,2)}} = m_{\rho_{(\bar{3},2)}} = y_2 v_\eta - \frac{y_3 v_\Xi v_\eta}{2\sqrt{30}\Lambda}. \tag{19}$$

Here m_{ρ_0}, m_{ρ_3} and m_{ρ_8} are the masses of the fermionic singlet ρ_0, triplet ρ_3 and octet ρ_8 contained in the **24** fermionic irrep of $SU(5)$, respectively. We denote by $m_{\rho_{(3,2)}}$ and $m_{\rho_{(\bar{3},2)}}$ the masses of the $(3, 2)$ and $(\bar{3}, 2)$ fermionic fields corresponding to the $SU(3)$ triplet and $SU(3)$ antitriplet, $SU(2)$ doublet parts of ρ, respectively. Consequently, the light active neutrino masses arise from type-I and type-III seesaw mechanisms induced by the $SU(5)$ singlet heavy Majorana neutrino N_R, the fermionic singlet ρ_0 and the fermionic triplet ρ_3, respectively.

From the neutrino Yukawa terms of Eq. (15) and the VEV pattern of the $SU(5)$ singlet T_7 scalar triplet χ given by Eq. (10), we find the neutrino mass matrix:

$$M_\nu = \begin{pmatrix} O_{3\times 3} & M_\nu^D \\ (M_\nu^D)^T & M_R \end{pmatrix},$$

$$M_\nu^D = \begin{pmatrix} 0 & Y_1 e^{-\frac{i\phi}{2}} & Y_2 e^{-\frac{i\phi}{2}} & Y_2 e^{-\frac{i\phi}{2}} & Y_2 e^{-\frac{i\phi}{2}} \\ X & 0 & 0 & 0 & 0 \\ 0 & Y_1 e^{\frac{i\phi}{2}} & Y_2 e^{\frac{i\phi}{2}} & Y_2 e^{\frac{i\phi}{2}} & Y_2 e^{\frac{i\phi}{2}} \end{pmatrix},$$

$$M_R = \begin{pmatrix} m_N & 0 & 0 & 0 & 0 \\ 0 & m_{\rho_0} & 0 & 0 & 0 \\ 0 & 0 & m_{\rho_3} & 0 & 0 \\ 0 & 0 & 0 & m_{\rho_3} & 0 \\ 0 & 0 & 0 & 0 & m_{\rho_3} \end{pmatrix}, \tag{20}$$

where

$$X = (\lambda_{1\nu} + \lambda_{2\nu}) v_H^{(1)} \frac{v_\chi^2}{\Lambda^2},$$
$$Y_1 = \frac{\sqrt{15}}{2}\left(\frac{1}{5}\lambda_{3\nu} v_H^{(1)} + \lambda_{4\nu} v_\Phi\right)\frac{v_\chi}{\Lambda},$$
$$Y_2 = (\lambda_{3\nu} v_H^{(1)} - 3\lambda_{4\nu} v_\Phi)\frac{v_\chi}{\Lambda}. \tag{21}$$

Therefore, the light neutrino mass matrix takes the following form:

$$M_L = M_\nu^D M_R^{-1} (M_\nu^D)^T = \begin{pmatrix} A e^{-i\phi} & 0 & A \\ 0 & B & 0 \\ A & 0 & A e^{i\phi} \end{pmatrix}, \tag{22}$$

where

$$A = \frac{Y_1^2}{m_{\rho_0}} + \frac{3Y_2^2}{m_{\rho_3}}, \qquad B = \frac{X^2}{m_N}. \tag{23}$$

The smallness of neutrino masses in our model is the consequence of their inverse scaling with respect to the large masses of the singlet ρ_0 and the triplet ρ_3 fermionic fields and proportionality to the squared neutrino Yukawa couplings.

The mass matrix M_L in Eq. (22) for light active neutrinos is diagonalized by a unitary rotation matrix V_ν. There are two solutions of this diagonalization problem:

$$V_\nu^\dagger M_L (V_\nu^\dagger)^T = \begin{pmatrix} m_1 & 0 & 0 \\ 0 & m_2 & 0 \\ 0 & 0 & m_3 \end{pmatrix}, \quad \text{with}$$

$$V_\nu = \begin{pmatrix} \cos\theta & 0 & \sin\theta e^{-i\phi} \\ 0 & 1 & 0 \\ -\sin\theta e^{i\phi} & 0 & \cos\theta \end{pmatrix} P_\nu,$$
$$\theta = \pm\frac{\pi}{4}, \tag{24}$$

$$P_\nu = \mathrm{diag}(e^{i\alpha_1/2}, e^{i\alpha_2/2}, e^{i\alpha_3/2}). \tag{25}$$

The solutions corresponding to $\theta = +\pi/4$ and $\theta = -\pi/4$ we identify with the normal (NH) and inverted (IH) neutrino mass hierarchies, respectively, so that

$$\text{NH: } \theta = +\frac{\pi}{4}: \; m_{\nu_1} = 0, \qquad m_{\nu_2} = B,$$
$$m_{\nu_3} = 2A, \qquad \alpha_1 = \alpha_2 = 0, \qquad \alpha_3 = \phi, \tag{26}$$

$$\text{IH: } \theta = -\frac{\pi}{4}: \; m_{\nu_1} = 2A, \qquad m_{\nu_2} = B,$$
$$m_{\nu_3} = 0, \qquad \alpha_2 = \alpha_3 = 0, \qquad \alpha_1 = -\phi. \tag{27}$$

Let us note the presence of nonvanishing Majorana phases ϕ and $-\phi$ for NH and IH cases, respectively. This simple relation requires the effective dimensionful parameters A and B, given by Eq. (23), to be real, which is consistent with our previously mentioned assumption that the dimensionless couplings in Eq. (15) are $\mathcal{O}(1)$ parameters assumed to be real, excepting $\gamma_{11}, \gamma_{12}, \gamma_{21}, \gamma_{31}$ and γ_{13}, assumed to be complex.

Now we find the Pontecorvo-Maki-Nakagawa-Sakata (PMNS) leptonic mixing matrix,

$$U = V_{lL}^\dagger V_\nu$$
$$= \begin{pmatrix} \frac{\cos\theta}{\sqrt{3}} - \frac{e^{i\phi}\sin\theta}{\sqrt{3}} & \frac{1}{\sqrt{3}} & \frac{\cos\theta}{\sqrt{3}} + \frac{e^{-i\phi}\sin\theta}{\sqrt{3}} \\ \frac{\cos\theta}{\sqrt{3}} - \frac{e^{i\phi+\frac{2i\pi}{3}}\sin\theta}{\sqrt{3}} & \frac{e^{-\frac{2i\pi}{3}}}{\sqrt{3}} & \frac{e^{\frac{2i\pi}{3}}\cos\theta}{\sqrt{3}} + \frac{e^{-i\phi}\sin\theta}{\sqrt{3}} \\ \frac{\cos\theta}{\sqrt{3}} - \frac{e^{i\phi-\frac{2i\pi}{3}}\sin\theta}{\sqrt{3}} & \frac{e^{\frac{2i\pi}{3}}}{\sqrt{3}} & \frac{e^{-\frac{2i\pi}{3}}\cos\theta}{\sqrt{3}} + \frac{e^{-i\phi}\sin\theta}{\sqrt{3}} \end{pmatrix} P_\nu, \tag{28}$$

with the pattern of the trimaximal (TM_2) type [61]. It is noteworthy that in our model the PMNS matrix depends on a single parameter ϕ, and the neutrino masses (26) and (27) depend on two parameters, A and B. Comparing the matrix U in Eq. (28) with the standard parameterization of the PMNS matrix in terms of the solar θ_{12}, the atmospheric θ_{23} and the reactor θ_{13} angles, we find

$$\sin^2\theta_{12} = \frac{|U_{e2}|^2}{1-|U_{e3}|^2} = \frac{1}{2 - z\cdot\cos\phi},$$
$$\sin^2\theta_{13} = |U_{e3}|^2 = \frac{1}{3}(1 + z\cdot\cos\phi),$$
$$\sin^2\theta_{23} = \frac{|U_{\mu 3}|^2}{1-|U_{e3}|^2} = \frac{2 - z\cdot(\cos\phi + \sqrt{3}\sin\phi)}{4 - 2z\cdot\cos\phi}, \quad (29)$$

with $z = 1$ and $z = -1$ for NH and IH, respectively. Note that in the limit $\phi = 0$ and $\phi = \pi$ for IH and NH, respectively, the mixing matrix in Eq. (28) reduces to the tribimaximal mixing pattern, which yields a vanishing reactor mixing angle θ_{13}.

For the Jarlskog invariant and the CP-violating phase [2], we find

$$J = \mathrm{Im}(U_{e1}U_{\mu 2}U_{e2}^{*}U_{\mu 1}^{*}) = -\frac{1}{6\sqrt{3}}\cos 2\theta = 0,$$
$$\sin\delta = \frac{8J}{\cos\theta_{13}\sin 2\theta_{12}\sin 2\theta_{23}\sin 2\theta_{13}} = 0, \quad (30)$$

since $\theta = \pm\frac{\pi}{4}$ according to Eq. (24).

Thus, our model predicts a vanishing leptonic Dirac CP-violating phase.

In what follows, we adjust the three free effective parameters ϕ, A and B of the active neutrino sector of our model to reproduce the experimental values of three leptonic mixing parameters and two neutrino mass-squared splittings, reported in Tables I and II, for the normal and inverted neutrino mass hierarchies, respectively. We fit the parameter ϕ to adjust the experimental values of the leptonic mixing parameters $\sin^2\theta_{ij}$, whereas A and B are fixed so that the measured mass-squared differences are reproduced for the normal (NH) and inverted (IH) neutrino mass hierarchies. From Eqs. (27), (26), and the definition $\Delta m_{ij}^2 = m_i^2 - m_j^2$, we find

$$\text{NH: } m_{\nu_1} = 0, \qquad m_{\nu_2} = B = \sqrt{\Delta m_{21}^2} \approx 9 \text{ meV},$$
$$m_{\nu_3} = 2|A| = \sqrt{\Delta m_{31}^2} \approx 50 \text{ meV}, \quad (31)$$

$$\text{IH: } m_{\nu_2} = B = \sqrt{\Delta m_{21}^2 + \Delta m_{13}^2} \approx 50 \text{ meV},$$
$$m_{\nu_1} = 2|A| = \sqrt{\Delta m_{13}^2} \approx 49 \text{ meV},$$
$$m_{\nu_3} = 0, \quad (32)$$

for the best-fit values of Δm_{ij}^2 taken from Tables I and II.

To fit the leptonic mixing parameters $\sin^2\theta_{ij}$ to their experimental values, given in Tables I and II, we vary the ϕ parameter, finding the following best fit result:

$$\text{NH: } \phi = -0.88\pi, \qquad \sin^2\theta_{12} \approx 0.34,$$
$$\sin^2\theta_{23} \approx 0.61, \qquad \sin^2\theta_{13} \approx 0.0232; \quad (33)$$

$$\text{IH: } \phi = 0.12\pi, \qquad \sin^2\theta_{12} \approx 0.34,$$
$$\sin^2\theta_{23} \approx 0.61, \qquad \sin^2\theta_{13} \approx 0.0238. \quad (34)$$

Thus, $\sin^2\theta_{13}$ is in excellent agreement with the experimental data, for both normal and inverted neutrino mass hierarchies, whereas $\sin^2\theta_{12}$ and $\sin^2\theta_{23}$ exhibit a 2σ deviation from their best-fit values.

Now we are ready to make a prediction for the neutrinoless double beta ($0\nu\beta\beta$) decay amplitude, which is proportional to the effective Majorana neutrino mass parameter,

$$m_{\beta\beta} = \left|\sum_k U_{ek}^2 m_{\nu_k}\right|, \quad (35)$$

where U_{ek}^2 and m_{ν_k} are the PMNS mixing matrix elements and the Majorana neutrino masses, respectively. Using Eqs. (24)–(28) and (31)–(34), we get for both normal and inverted hierarchies

$$m_{\beta\beta} = \frac{1}{3}\left(B + 4A\cos^2\frac{\phi}{2}\right) = \begin{cases} 4 \text{ meV} & \text{for NH,} \\ 50 \text{ meV} & \text{for IH.} \end{cases} \quad (36)$$

These values are beyond the reach of the present and forthcoming $0\nu\beta\beta$ decay experiments. The presently best upper limit on the effective neutrino mass is $m_{\beta\beta} \leq 160$ meV, which arises from the recently quoted EXO-200 experiment [62] $T_{1/2}^{0\nu\beta\beta}(^{136}\mathrm{Xe}) \geq 1.6\times 10^{25}$ yr at 90% C.L. This limit will be improved within the not-too-distant future. The GERDA "phase II" experiment [63,64] is expected to reach $T_{1/2}^{0\nu\beta\beta}(^{76}\mathrm{Ge}) \geq 2\times 10^{26}$ yr, corresponding to $m_{\beta\beta} \leq 100$ meV. A bolometric CUORE experiment, using ^{130}Te [65], is currently under construction. It has an estimated sensitivity around $T_{1/2}^{0\nu\beta\beta}(^{130}\mathrm{Te}) \sim 10^{26}$ yr, which corresponds to $m_{\beta\beta} \leq 50$ meV. There are also proposals for ton-scale next-to-next-generation $0\nu\beta\beta$ experiments with ^{136}Xe [66,67] and ^{76}Ge [63,68] claiming sensitivities over $T_{1/2}^{0\nu\beta\beta} \sim 10^{27}$ yr, corresponding to $m_{\beta\beta} \sim$ 12–30 MeV. For recent reviews, see for example Ref. [69]. Consequently, as can be seen from Eq. (36), our model predicts $T_{1/2}^{0\nu\beta\beta}$ at the level of sensitivities of the next-generation or next-to-next-generation $0\nu\beta\beta$ experiments.

IV. QUARK MASSES AND MIXING

Using Eq. (15), together with the product rules for the T_7 group given in Appendix A, and considering that the components of the $SU(5)$ singlet T_7 scalar triplet ξ acquire the same VEV as shown by Eq. (10), which is set to be

equal to $\lambda\Lambda$ as the VEV of the Z_{12} charged scalar σ as indicated by Eq. (12) (Λ being the cutoff of our model), we find the quark mass matrices:

$$M_U = \begin{pmatrix} a_{11}^{(U)}\lambda^6 & a_{12}^{(U)}\lambda^5 & a_{13}^{(U)}\lambda^3 \\ a_{12}^{(U)}\lambda^5 & a_{22}^{(U)}\lambda^4 & a_{23}^{(U)}\lambda^2 \\ a_{13}^{(U)}\lambda^3 & a_{23}^{(U)}\lambda^2 & a_{33}^{(U)} \end{pmatrix} \frac{v}{\sqrt{2}}, \tag{37}$$

$$\begin{aligned} M_D &= \frac{v}{\sqrt{2}} \begin{pmatrix} a_1^{(D)}\lambda^8 & 0 & 0 \\ 0 & a_2^{(D)}\lambda^5 & 0 \\ 0 & 0 & a_3^{(D)}\lambda^3 \end{pmatrix} (V_{lL}^{\dagger})^T \\ &= \mathrm{diag}(m_d, m_s, m_b)(V_{lL}^{\dagger})^T, \end{aligned} \tag{38}$$

where $\lambda = 0.225$ and the $\mathcal{O}(1)$ dimensionless couplings in Eqs. (37) and (38) are given by

$$\begin{aligned} a_{12}^{(U)} &= 2\sqrt{2}(\gamma_{12} + \gamma_{21})\frac{v_H^{(4)}}{v}, \\ a_{11}^{(U)} &= 4\sqrt{2}\gamma_{11}\frac{v_H^{(2)}}{v}, \\ a_{13}^{(U)} &= 2\sqrt{2}(\gamma_{13} + \gamma_{31})\frac{v_H^{(3)}}{v}, \\ a_{23}^{(U)} &= 2\sqrt{2}(\gamma_{23} + \gamma_{32})\frac{v_H^{(2)}}{v}, \\ a_{22}^{(U)} &= 4\sqrt{2}\gamma_{22}\frac{v_H^{(3)}}{v}, \\ a_{33}^{(U)} &= 4\sqrt{2}\gamma_{33}\frac{v_H^{(4)}}{v}, \\ a_1^{(D)} &= \frac{1}{v}(\alpha_1 v_H^{(1)} + 2\beta_1 v_\Phi), \\ a_2^{(D)} &= \frac{1}{v}(\alpha_2 v_H^{(1)} + 2\beta_2 v_\Phi), \\ a_3^{(D)} &= \frac{1}{v}(\alpha_3 v_H^{(1)} + 2\beta_3 v_\Phi). \end{aligned} \tag{39}$$

From Eq. (38) it follows that the CKM quark mixing matrix does not receive contributions from the down-type quark sector, meaning that quark mixing arises solely from the up-type quark sector. Consequently, having realistic up-type quark masses and quark mixing angles requires that the mass matrix for up-type quarks be given by

$$M_U = V_{\mathrm{CKM}}\mathrm{diag}(m_u, m_c, m_t)V_{\mathrm{CKM}}^T. \tag{40}$$

Using the standard parametrization for the CKM quark mixing matrix, together with the relations $m_u = a\lambda^8 m_t$ and $m_c = b\lambda^4 m_t$, where a and b are $\mathcal{O}(1)$ coefficients, we get the mass matrix for up-type quarks described in Eq. (37), with entries exhibiting different scalings in terms of powers of the Wolfenstein parameter $\lambda = 0.225$. Thus, from the requirement of realistic up-quark masses and quark mixing angles with $\mathcal{O}(1)$ dimensionless couplings in Eq. (37), we find a λ^6 suppression in the 11 entry of the up-quark mass matrix instead of a λ^8 one. We have numerically checked that a λ^6 supression in the 11 entry of the up-quark mass matrix, with $\mathcal{O}(1)$ dimensionless couplings, is consistent with realistic up-quark masses and quark mixing angles.

Assuming that the quark mass and mixing pattern is caused by the breaking of the Z_3, Z_4 and Z_{12} symmetries, to simplify our analysis, we adopt a benchmark where the dimensionless charged fermion Yukawa couplings are approximately equal. Specifically, we set

$$\begin{aligned} \gamma_{11} &= \left(1 - \frac{\lambda^2}{2}\right)^{1/2}\gamma_1 e^{i\phi_1}, \\ \gamma_{12} &= \gamma_{21} = -\gamma_1 e^{i\phi_2}, \\ \gamma_{22} &= \gamma_1\left(1 - \frac{\lambda^2}{2}\right)^{-1/2}, \\ \gamma_{13} &= \gamma_{31} = \gamma_2\left(1 - \frac{\lambda^2}{2}\right)^{3} e^{i\phi_3}, \\ \gamma_{23} &= \gamma_{32} = -\gamma_2, \\ \alpha_i &= \beta_i, \qquad i = 1, 2, 3, \end{aligned} \tag{41}$$

with γ_1, γ_2, α_i and β_i ($i = 1, 2, 3$) real $\mathcal{O}(1)$ parameters. Our benchmark of nearly equal charged fermion Yukawa couplings given in Eq. (41), which we have numerically checked is consistent with realistic up-quark masses and quark mixing angles, is also adopted in order to reduce the number of free effective parameters in the quark sector of our model. There is no tuning in the parameters of our model. Let us note that the exactly equal dimensionless quark Yukawa couplings do not allow generating the up- and charm-quark masses. In Appendix B we give another possible motivation for the approximate universality of dimensionless couplings, which can be studied beyond the present model, adding new symmetries.

Besides that, for simplicity we assume that the complex phase responsible for CP violation in the quark sector arises solely from the up-type quark sector, as indicated by Eq. (41). In addition, to simplify the analysis, we fix $a_{33}^{(U)} = 1$, as suggested by naturalness arguments. Consequently, the up-type quark mass matrix reads

$$M_U = \begin{pmatrix} a_1^{(U)}\left(1-\frac{\lambda^2}{2}\right)^{1/2}\lambda^6 e^{i\phi_1} & -a_1^{(U)}\lambda^5 e^{i\phi_2} & a_2^{(U)}\left(1-\frac{\lambda^2}{2}\right)^{3}\lambda^3 e^{i\phi_3} \\ -a_1^{(U)}\lambda^5 e^{i\phi_2} & a_1^{(U)}\left(1-\frac{\lambda^2}{2}\right)^{-1/2}\lambda^4 & -a_2^{(U)}\lambda^2 \\ a_2^{(U)}\left(1-\frac{\lambda^2}{2}\right)^{3}\lambda^3 e^{i\phi_3} & -a_2^{(U)}\lambda^2 & 1 \end{pmatrix}\frac{v}{\sqrt{2}}, \quad (42)$$

As seen from the above formulas, the quark sector of our model contains ten parameters—i.e, λ, $a_{33}^{(U)}$, $a_1^{(U)}$, $a_2^{(U)}$, $a_1^{(D)}$, $a_2^{(D)}$, $a_3^{(D)}$, and the phases ϕ_l $(l = 1, 2, 3)$—to describe the quark mass and mixing pattern, which is characterized by ten physical observables—i.e., the six quark masses, the three mixing angles and the CP phase. Out of the ten model parameters, two of them, λ and $a_{33}^{(U)}$, are fixed, whereas the remaining eight are fitted to reproduce the six quark masses and four quark mixing parameters. In Table III we show the experimental values of the physical observables in the quark sector, together with our results obtained for the following best-fit values of the model parameters:

$$\begin{aligned} &a_1^{(U)} \simeq 1.96, \quad a_2^{(U)} \simeq 0.74, \quad \phi_1 \simeq 10.94°, \\ &\phi_2 \simeq 6.02°, \quad \phi_3 \simeq 21.65°, \\ &a_1^{(D)} \simeq 2.54, \quad a_2^{(D)} \simeq 0.58, \quad a_3^{(D)} \simeq 1.42. \end{aligned} \quad (43)$$

TABLE III. Model and experimental values of the quark masses and CKM parameters.

Observable	Model value	Experimental value
m_u (MeV)	0.86	$1.45^{+0.56}_{-0.45}$
m_c (MeV)	673	635 ± 86
m_t (GeV)	174.2	$172.1 \pm 0.6 \pm 0.9$
m_d (MeV)	2.9	$2.9^{+0.5}_{-0.4}$
m_s (MeV)	57.7	$57.7^{+16.8}_{-15.7}$
m_b (GeV)	2.82	$2.82^{+0.09}_{-0.04}$
$\lvert V_{ud}\rvert$	0.974	0.97427 ± 0.00015
$\lvert V_{us}\rvert$	0.2257	0.22534 ± 0.00065
$\lvert V_{ub}\rvert$	0.00305	$0.00351^{+0.00015}_{-0.00014}$
$\lvert V_{cd}\rvert$	0.2256	0.22520 ± 0.00065
$\lvert V_{cs}\rvert$	0.97347	0.97344 ± 0.00016
$\lvert V_{cb}\rvert$	0.0384	$0.0412^{+0.0011}_{-0.0005}$
$\lvert V_{td}\rvert$	0.00785	$0.00867^{+0.00029}_{-0.00031}$
$\lvert V_{ts}\rvert$	0.0377	$0.0404^{+0.0011}_{-0.0005}$
$\lvert V_{tb}\rvert$	0.999145	$0.999146^{+0.000021}_{-0.000046}$
J	2.32×10^{-5}	$(2.96^{+0.20}_{-0.16}) \times 10^{-5}$
δ	64°	68°

We use the experimental values for the quark masses at the M_Z scale, reported in Ref. [70] (which are similar to those in Ref. [71]), whereas the experimental values of the CKM matrix elements, the Jarlskog invariant J and the CP-violating phase δ are taken from Ref. [2]. Let us note that the agreement of our model with the experimental data is as good as in the models of Refs. [72–79], and better than in Refs. [31,80–87]. The following comparison of our model with these models could be in order. Despite the similar quality of the data description, our model is more predictive than the model of Ref. [72], since the latter, focused only on the quark sector, has a total of 12 free parameters, whereas the quark sector of our model is described by 8 free effective parameters that are adjusted to reproduce the 10 physical observables of the quark sector. The models of Ref. [75], Ref. [73,80], Ref. [82], Refs. [79,81,87], Refs. [74,76–78,85], Refs. [84,86], and Ref. [83] possess in the quark sector 6, 7, 8, 9, 10, 12, and 13 free parameters. The total number of the effective free parameters of our T_7 flavor adjoint $SU(5)$ GUT model is 16, from which 2 are fixed and 14 are fitted to reproduce the experimental values of 18 observables in the quark and lepton sectors. On the other hand, the $SU(5)$ model with $T' \otimes Z_{12} \otimes Z'_{12}$ symmetry of Ref. [31] has nine parameters in the Yukawa sector for the charged fermions and the neutrinos. However, it does not account for CP violation in the quark sector, whereas our model does. Furthermore, the values of the physical observables we derived in our model for both quark and lepton sectors exhibit a significantly better agreement with their corresponding experimental values than those derived in Ref. [31] within the $SU(5)$ model with $T' \otimes Z_{12} \otimes Z'_{12}$ symmetry.

V. GAUGE COUPLING $SU(5)$ UNIFICATION

In the previous sections, we analyzed the possibility of describing the quark and lepton masses and flavor mixing within the framework of our model. This analysis was based on the symmetries of the model and particular field assignments to the symmetry group representations, which allowed us to single out several effective parameters completely determining the lepton and quark mass matrices. It is a notable property of the model that the SM fermion mass matrices depend on the "fundamental" parameters of the model Lagrangian only through this set of a few effective parameters. Now we turn to more subtle aspects of the model depending on the details of the

non-SM components of the $SU(5)$ multiplets, as well as on the "fundamental" parameters, which may have crucial impact on its ultraviolet behavior.

As is well known, there are many extensions of the SM which lead to gauge coupling unification (GCU) and also successfully fulfill all the constraints coming from fermion masses, proton decay, and perturbativity. In particular, models based on supersymmetric and also nonsupersymmetric (non-SUSY) $SU(5)$ unification have been widely studied in the literature [42,88]. For non-SUSY $SU(5)$ scenarios, the unification of gauge couplings can be as good as or better than in the MSSM, despite the fact that the number of extra fields beyond the SM is smaller. More restrictive conditions such as the possibility of implementation of an appropriate neutrino mass generation mechanism, and compatibility with the existing phenomenological, cosmological and astrophysical constraints, require some specific properties for this extra field content. As was already pointed out in Sec. II, the $SU(5)$ scalar representations with the minimal number of Higgs bosons needed to generate the fermions masses and mixings are one $\mathbf{24}_s$, one $\mathbf{45}_s$, four $\mathbf{5}_s$'s, and twelve $\mathbf{1}_s$'s. If an extra fermionic $\mathbf{24}_f$ representation is also included, a simple configuration of the extra fields allowing the type-I and type-III seesaw mechanisms of neutrino mass generation can be constructed with masses below the GUT scale. As will be shown later, the condition of the GCU and compatibility with the lower experimental limit on the proton decay half-life predicts the masses for the extra scalar fields within the LHC reach. This opens up the possibility for experimental tests of the considered models. On the other hand, the dark matter constraints on the scalar sector will lead us to the conclusion that the masses for the type-I and type-III fermionic seesaw mediators, $m_{\rm NR}$, m_{ρ_0} and m_{ρ_3}, should be at high energies far beyond the TeV ballpark.

It is noteworthy to mention that our configurations rely on fine-tuning which separates light from heavy degrees of freedom. However, this issue is an unavoidable problem of grand unified theories. Evidence of this is the standard $SU(5)$, which suffers from what is known as the doublet-triplet splitting problem—i.e., the fact that the SM Higgs doublet has a mass of $m_h \sim 125$ GeV while the colored triplet in the 5 irrep must have a mass of the order of the GUT scale in order to prevent proton decay. Although several solutions to this problem have been suggested in the literature (for a short review, see Ref. [89]), we do not consider here any particular one. Instead, we view this as a fine-tuning problem and, in fact, to make the exotic particles in our model light will require, in general, additional fine-tunings. We assured ourselves that the large number of free and uncorrelated parameters in the scalar potential will allow us to reproduce the required mass differences. There are non-SUSY $SU(5)$ models which also heavily rely on fine-tuning among states, and which do not consider formal solutions to this problem, as seen in Refs. [30,42]. We are aware of this fine-tuning problem, whose formal solution goes beyond the scope of this work and is deferred for a future publication.

A. Setup

The scalar sector of our model is composed, as described in the previous sections, by the $\mathbf{5}_s$, $\mathbf{24}_s$, and $\mathbf{45}_s$ irreps of $SU(5)$ with the following $SU(3)_C \times SU(2)_L \times U(1)_Y$ decompositions:

$$\begin{aligned}
\mathbf{5}_s &= (1,2)_{1/2} \oplus (3,1)_{-1/3}, \\
&= H_1 \oplus H_2, \\
\mathbf{24}_s &= (1,1)_0 \oplus (1,3)_0 \oplus (8,1)_0 \oplus (3,2)_{-5/6} \oplus (\bar{3},2)_{5/6}, \\
&= \Xi_1 \oplus \Xi_3 \oplus \Xi_8 \oplus \Xi_{(3,2)} \oplus \Xi_{(\bar{3},2)}, \\
\mathbf{45}_s &= (1,2)_{1/2} \oplus (3,1)_{-1/3} \oplus (3,3)_{-1/3} \oplus (\bar{3},1)_{4/3} \\
&\quad \oplus (\bar{3},2)_{-7/6} \oplus (6,1)_{-1/3} \oplus (8,2)_{1/2}, \\
&= \Phi_1 \oplus \Phi_2 \oplus \Phi_3 \oplus \Phi_4 \oplus \Phi_5 \oplus \Phi_6 \oplus \Phi_7. \qquad (44)
\end{aligned}$$

The SM Higgs doublet is embedded in the $\mathbf{5}_s$. The adjoint $\mathbf{24}_s$ representation triggers the breaking of $SU(5)$ to the SM at the GUT scale. As we previously commented, this particle content should be further extended in order to account for the nonzero neutrino masses. We introduced a fermionic $\mathbf{24}_f$ irrep of the $SU(5)$. It has the SM decomposition

$$\begin{aligned}
\mathbf{24}_f &= (1,1)_0 \oplus (1,3)_0 \oplus (8,1)_0 \oplus (3,2)_{-5/6} \oplus (\bar{3},2)_{5/6} \\
&= \rho_0 \oplus \rho_3 \oplus \rho_8 \oplus \rho_{(3,2)} \oplus \rho_{(\bar{3},2)}. \qquad (45)
\end{aligned}$$

In this case the $SU(5)$ singlet N_R Majorana neutrino with the heavy SM singlet ρ_0 mediate type-I seesaw mechanism while the $SU(2)_L$ triplet ρ_3 gives rise to the type-III seesaw mechanism. Combining these three extra fermions, N_R, ρ_0, and ρ_3, with some of the scalar fields from the $\mathbf{5}_s$, $\mathbf{24}_s$, and $\mathbf{45}_s$ irreps, we construct the simplest benchmark configurations that unify the gauge couplings within the $SU(5)$ and satisfy some general requirements in order to guarantee their phenomenological viability. These requirements are

(i) *Perturbative $SU(5)$ unification:* This means that gauge couplings unify as well as or even better than in the MSSM, and the value of α_G is in the perturbative regime. Note that we are not necessarily imposing the exact unification of the gauge couplings at the GUT scale (m_G). Rather, we allow for a difference of the gauge couplings at m_G falling into the area of the MSSM "nonunification triangle" [90,91].

(ii) *Proton decay:* There are some specific fields contributing to proton decay. The dimension-six proton decay operators are mediated by the superheavy

gauge bosons, usually named leptoquarks, in the **24** irrep: $\rho_{(3,2)} \oplus \rho_{(\bar{3},2)} = (3,2,-5/6) \oplus (\bar{3},2,5/6)$, which must be heavier than 3×10^{15} GeV to satisfy the experimental lower bound on the proton decay lifetime. Here, we assume that these fields live at the GUT scale. In addition, we deal with field configurations which, in almost all the parameter space, fulfill the current constraint from $\tau_{p\to\pi^0 e^+} \gtrsim 10^{34}$ years [92,93]. This, through the relation for the proton decay half-life, $\Gamma = \alpha_G^2 m_p^5/m_G^4$, leads to a GUT scale of $m_G \gtrsim 3 \times 10^{15}$ GeV.

(iii) *Fermion masses:* In particular, neutrino mass generation through the type-I and type-III seesaw mechanisms [41,94]. The configurations should then contain at least one copy of the fermionic fields N_R, ρ_0, and ρ_3, as described before.

(iv) *Nontrivial phenomenology:* Among the models passed through the above three conditions, we select those models which may provide a distinguishing signal at the LHC.

In what follows, we analyze some of the "minimal" benchmark models, which lead to correct unification and also fulfill the above listed requirements, with as simple a field content as possible. As the preferable models, we consider those which are phenomenologically rich enough, in the sense that some of the fields (being colored) could give rise to certain resonances at the LHC. The analyzed models will lead to an available parameter space for the different masses of the scalars and the type-I, type-III seesaw fermionic mediators.

B. The models

For simplicity, and following the notations of Ref. [43], we rewrite the masses of the fermionic $\mathbf{24}_f$ given in Eq. (19) as follows:

$$\begin{aligned} m_{\rho_3} &= m - 3e^{i\alpha}\Lambda', \\ m_{\rho_8} &= m + 2e^{i\alpha}\Lambda', \\ m_{\rho_{(3,2)}} &= m_{\rho_{(\bar{3},2)}} = m - 1/2e^{i\alpha}\Lambda', \\ m_{\rho_0} &= m - e^{i\alpha}\Lambda', \end{aligned} \tag{46}$$

where α is the relative phase between y_2 and y_3. For the particular case where $\alpha = 0$, the parameters Λ' and m are then defined as $m = y_2 v_\eta$ and $\Lambda' = \hat{y}_3 v_\Xi \frac{v_\eta}{\Lambda}$ (where $\hat{y}_3 = y_3/\sqrt{30}$).

In order to deal with the simplest models, we look for configurations where the only contribution from the fermionic $\mathbf{24}_f$ to the RGE flow comes from the fermionic type-I and type-III seesaw mediators. We assume the other $\mathbf{24}_f$ components, ρ_8, $\rho_{(3,1)}$, and $\rho_{(\bar{3},2)}$, have no RGE effect, being as heavy as the GUT scale. It is worth reiterating that in the analyzed benchmark models the GCU is achieved having a few particles with masses below the GUT scale: the fermions N_R, ρ_0, ρ_3 plus some of the extra scalar fields from the $\mathbf{5}_s$, $\mathbf{24}_s$, and $\mathbf{45}_s$ multiplets. This kind of spectra can be easily obtained by fine-tuning Eq. (46), imposing that the mass of the remaining fermionic fields in the $\mathbf{24}_f$ lives at the GUT scale or above.

Searching for the models, we keep our analysis at the one-loop level. It could be easily extended to two loops. However, this sophistication makes no impact on our final results and conclusions.

The master equation for the running of the inverse gauge couplings at the one-loop level is

$$\alpha_i^{-1}(\mu) = \alpha_i^{-1}(\mu_0) - \frac{b_i^{\rm eff}(\mu)}{2\pi}\ln\left(\frac{\mu}{\mu_0}\right), \quad \text{with} \quad i = 1,2,3. \tag{47}$$

The effective one-loop RGE coefficients, taking into account the thresholds from particles with masses m_f, are given by

$$b_i^{\rm eff}(\mu) = \sum_f \theta(\mu - m_f) b_i^f. \tag{48}$$

The contribution of each particle b_i^f is calculated according to

$$b_i = -\frac{11}{3}T_i(R_G) + \frac{2}{3}T_i(R_F) + \frac{1}{3}T_i(R_B). \tag{49}$$

where $T(R_I)$ are the Dynkin indexes of the representations R_I to which belong $I = G$, F, and B—the gauge bosons, fermions, and scalars, respectively. They are defined as $T(R)\delta_{mn} = \mathrm{Tr}(T_m(R)T_n(R))$, with $T_m(R)$ being generators in the representation R. For the lowest-dimension representations of $SU(N)$ they are $T(\text{fundamental}) = 1/2$, $T(\text{Adj}) = N$. For the SM we have $(b_3^{\rm SM}, b_2^{\rm SM}, b_1^{\rm SM}) = (-7, -19/6, 41/10)$, which correspond to the contributions of the SM fermions and one copy of the $SU(2)_L$ Higgs doublet. The additional non-SM fields introduce extra contributions $\Delta b_i'$ to these coefficients $b_i = b_i^{\rm SM} + \Delta b_i'$. In Table IV (Appendix C), the $\Delta b_i'$ contributions of the fields in the 5_S, 10_S, 24_S, 24_f, and 45_S $SU(5)$ representations are shown. In order to correctly unify the gauge couplings and fulfill all the requirements *(i)–(iv)* in Sec. V A, which we impose on the models, these $\Delta b_i'$ coefficients should obey certain conditions. Some of the simplest configurations of the non-SM fields with the masses below the GUT scale, which obey these conditions, are listed in Table V (Appendix C). All the listed field configurations have a highly split mass spectrum with type-I, type-III seesaw mediators at $m_S \sim 10^{14}$ GeV and remaining scalars at $m_{\rm NP} = 2$ TeV. Let us note that since among the scalars there are the color octets, we use

2 TeV as a limit recently established on the mass of color octets by the CMS and ATLAS collaborations [95] from the dijet pair signature searches. We have purposely chosen the latter scale to be low enough so that the colored scalars are within the LHC's mass reach, while the large value for the seesaw scale m_S is in agreement with the small neutrino masses. Let us consider two simplest models (1) and (2) from Table V: *Model (1):* This is the simplest of all the benchmark models passing our conditions *(i)–(iv)* in Sec. V A, including the unification of the gauge couplings and smallness of neutrino masses. However, if we fix the masses of the scalar fields $\Xi_{3,8}$ at $m_{\rm NP} = 2$ TeV and the fermionic seesaw mediators $\rho_{0,3}$, N_R at $m_S = 10^{14}$ GeV, as is done for all the models in Table V, we get the GUT scale $m_G = 2.7 \times 10^{15}$ GeV, which is in slight tension with the limit imposed by the proton stability $m_G \gtrsim 3 \times 10^{15}$ GeV. This flaw can easily be cured by allowing the masses of the fields to vary independently in the range $2\ \text{TeV} \leq m_{\Xi 3}$, $m_{\Xi 8} \leq m_S < m_G$. Now, as shown in Fig. 1, a significant part of the model parameter space corresponds to the GUT scale in the range allowed by the proton decay constraint. From the left panel of this figure, we can see that in this part of the parameter space the masses m_S of the seesaw mediators $\rho_{0,3}$, N_R could be in the ballpark of $[10^{8.5}, 10^{15.5}]$ GeV. The right panel of Fig. 1 shows that in the part of the parameter space consistent with the proton decay constraints, the mass of the scalar octet Ξ_8 is relatively low, $2\ \text{TeV} < m_{\Xi_8} \lesssim 10^6$ GeV. Thus, there is a chance for Ξ_8 to be within the mass reach of the current run of the LHC. However, its production cross section suffers from several suppression factors. The process of single-Ξ_8 production is only possible in the gluon fusion $gg \to \Xi_8$ via a loop with two or three internal Ξ_8, which is suppressed by the large m_{Ξ_8}. On the other hand, as seen from Eq. (15), it cannot be produced in $q\bar{q} \to \Xi_8$. The tree-level pair production process $gg \to \Xi_8\Xi_8$, being not suppressed in the amplitude, has a high threshold of $2m_{\Xi_8}$. If produced, Ξ_8 decays in a unique channel $\Xi_8 \to gg$. However, the corresponding signal at the LHC could be challenging from the viewpoint of the identification of its origin. Below we consider another benchmark model with a more distinctive signature of the color octet from **45**.

A viable dark matter (DM) candidate in non-SUSY models is an issue requiring special efforts. References [43,96] recently proposed the neutral component Ξ^0 of the $\Xi_3 \sim (1,3)_0 \subset \mathbf{24}_s$ as a scalar cold dark matter (CDM) candidate. The necessary condition for its stability is the vanishing of the trilinear coupling of $H^\dagger \Xi_3 H$ with the SM Higgs doublet, H. Also, its VEV must be zero, $\langle \Xi^0 \rangle = 0$. These conditions, as shown in Ref. [43], can be implemented by an *ad hoc* fine-tuning of

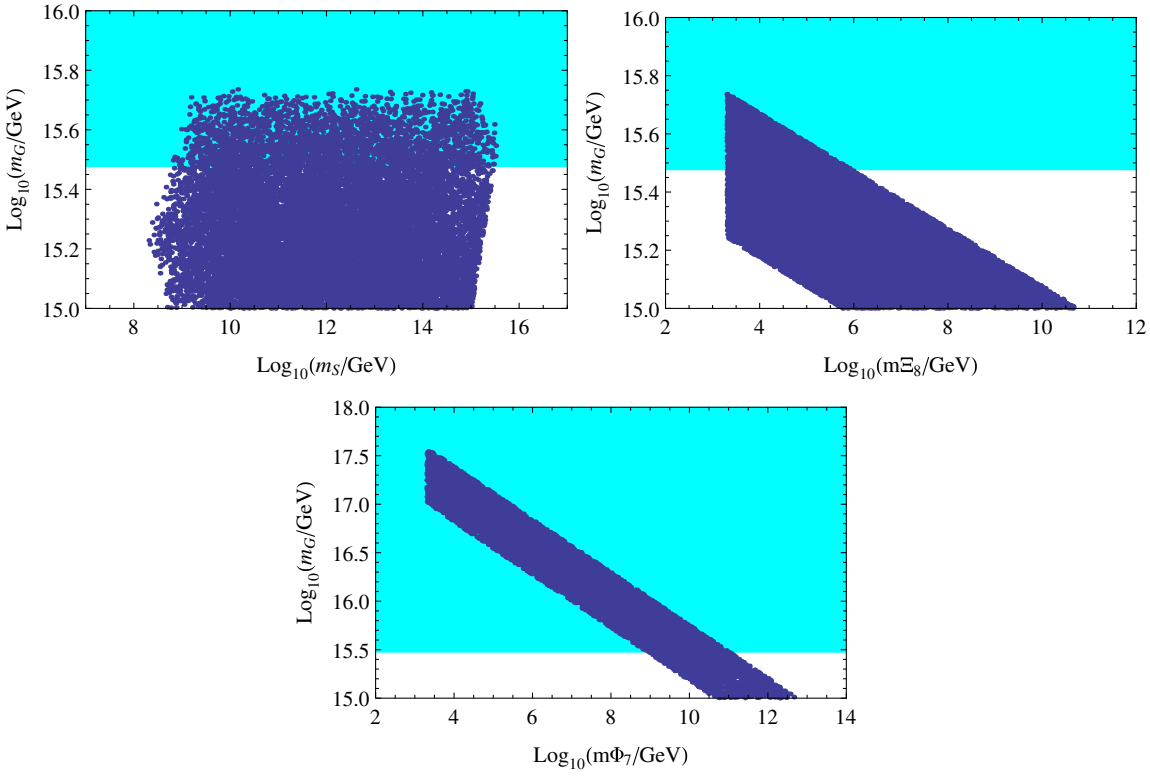

FIG. 1 (color online). The parameter space passing the conditions *(i)–(iv)* in Sec. V A. The region compatible with the proton decay constraints $m_G \geq 3 \times 10^{15}$ GeV is explicitly shown in light blue. The upper two panels correspond to *Model (1)* and the lower one to *Model (2)* considered in the text. In the latter case, the mass of the extra scalar electroweak doublet Φ_1 is fixed at 2 TeV.

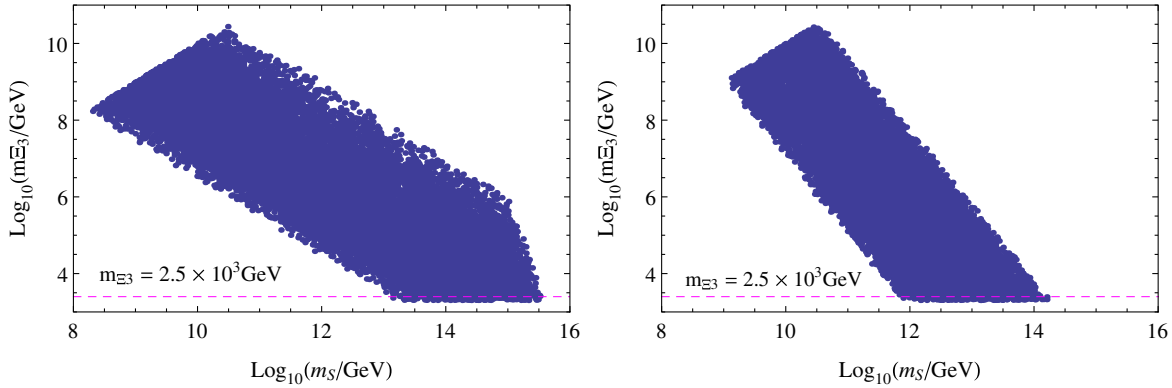

FIG. 2 (color online). Dark matter constraints: allowed parameter space in m_S and m_{Ξ_3}. The left and right panels correspond to *Models (1)* and *(2)*, respectively.

the scalar potential parameters. Unfortunately, no proper custodial symmetry, protecting this fine-tuning, can be incorporated in the adjoint $SU(5)$ framework [43]. Despite this complication, we study constraints on our model from the assumption that the Ξ^0 is a CDM candidate. It has been shown in Ref. [96] that the thermal relic abundance could be compatible with the observed DM abundance $\Omega_{\rm DM}h^2 = 0.110 \pm 0.005$, if $m_{\Xi_3} \sim 2.5$ TeV. We use this fixed value as a condition allowing the presence of a viable CDM particle candidate Ξ^0 in the model. In Fig. 2 we show limitations on the model parameter space, taking into account this condition. As seen, the lowest bound on the seesaw mediator mass is $m_S \gtrsim 10^{13}$ GeV. This large value of the seesaw mass scale perfectly accounts for the smallness of the neutrino masses. *Model (2):* This is the next simplest benchmark model from Table V. It contains a scalar color octet $\Phi_7 \sim (8,2)_{1/2} \subset \mathbf{45}$. Its production and possible signals at the LHC have been studied in Ref. [97] (for the earlier studies of the color octet scalars at the LHC see, for instance, Ref. [98]). The neutral and charged components $S^0_{R,I}$, $S^{\pm}$ of this multiplet, unlike the Ξ_8 in *Model (1)*, can be singly produced at tree level in quark-antiquark annihilation $q\bar{q} \to S^0_{R,I}$, $q'\bar{q} \to S^{\pm}$ and in the gluon fusion at one-loop level via b-quark loop, which is much less suppressed than the loop-induced production of a single Ξ_8. The tree-level pair production, dominated by the gluon fusion $gg \to S^0S^0$, $S^{\pm}S^{\mp}$, is approximately an order of magnitude smaller than the single-S production at $m_S \sim 2$ TeV, according to Ref. [97]. However, the single-S production cannot overcome the SM background with all the versatile kinematical cuts applied in Ref. [97], and therefore has no observational prospects. On the other hand, it has been shown that the S-pair production, even having a smaller production cross section, may get larger than the background in the $4b$-tagged final-state jets with a cut $P_T \geq 800$ GeV.

Repeating the analysis made for the previous model, we find masses m_{Φ_7} compatible with the proton decay constraints $m_G \geq 3 \times 10^{15}$ GeV. As shown in Fig. 1, we have $2\ \text{TeV} < m_{\Phi 7} \lesssim 10^{11}$ GeV.

Let us note also that, even if we fix the mass of all the scalars at 2 TeV and the seesaw mediators at 10^{14} GeV, as is done for the models in Table V, the GUT scale is still high enough to be safe, facing new possible improvement of the proton decay constraints in the future experiments. Now, as with *Model (1)*, we consider the constraints imposed on the present model by the interpretation of the Ξ_3 as a CDM candidate. As we discussed above, this requires that $m_{\Xi_3} \sim 2.5$ TeV. Scanning the parameter space, as with *Model (1)*, we find the plot shown in the right panel of Fig. 2, from which we derive the lower bound $m_S \gtrsim 10^{12}$ GeV.

VI. CONCLUSIONS AND DISCUSSION

We proposed a version of the adjoint $SU(5)$ grand unification model with an extra $T_7 \otimes Z_2 \otimes Z_3 \otimes Z_4 \otimes Z'_4 \otimes Z_{12}$ flavor symmetry, which successfully describes the SM fermion mass and mixing pattern. The model has in total 16 effective free parameters, from which 2 are fixed and 14 are fitted to reproduce the experimental values of 18 observables in the quark and lepton sectors—i.e., 9 charged fermion masses, 2 neutrino mass-squared splittings, 3 lepton mixing parameters, 3 quark mixing angles, and 1 CP-violating phase of the CKM quark mixing matrix. The observed hierarchy of charged fermion masses and quark mixing angles is a consequence of the $Z_3 \otimes Z_4 \otimes Z_{12}$ symmetry breaking, triggered by the $SU(5)$ scalar singlets σ, τ, and φ, charged under this symmetry, and which acquire VEVs at a very high-energy scale, close to the GUT scale. The non-SM fermion spectrum of our model is composed of a single heavy $SU(5)$ singlet right-handed Majorana neutrino N_R and two more fermionic fields: an electroweak singlet ρ_0 and triplet ρ_3, both from the adjoint

24 irrep of $SU(5)$. Thus the light neutrino masses arise in our model from type-I and type-III seesaw mechanisms mediated by these fields. The smallness of neutrino masses is a consequence of their inverse scaling with respect to the masses of these three seesaw mediators as well as the quadratic proportionality to the presumably small neutrino Yukawa couplings. The model predictions for the physical parameters in the quark and lepton sectors are in good agreement with the experimental data. The experimentally observed deviation from the trimaximal pattern is implemented by introducing two T_7 triplet scalars χ and ξ, singlets under $SU(5)$. The model predicts an effective Majorana neutrino mass, relevant for neutrinoless double beta decay, with values $m_{\beta\beta} = 4$ and 50 meV, for the normal and the inverted neutrino spectrum, respectively. In the latter case, our prediction is within the declared reach of the next-generation bolometric CUORE experiment [65] or, more realistically, of the next-to-next-generation tone-scale $0\nu\beta\beta$-decay experiments.

According to our model, the leptonic Dirac CP-violating phase is vanishing. In view of the current experimental trend, it could get into tension with the observations. The latest fit of the neutrino oscillation experimental data by the Valencia group, Ref. [8], indicates a nonvanishing CP-violating phase at the 1σ (less than 2σ) level for the normal (inverted) neutrino mass hierarchy. The Bali group in their fits claims slightly larger significance, but also below the 3σ level [99]. Thus, with the current experimental significance, essentially below than the golden 5σ, our model is not yet in trouble with the CP. On the other hand, we are aware of the necessity of reconsidering this aspect of our approach, which will be done elsewhere.

In the last section of this paper, we studied the compatibility of our model with certain physical conditions expected from a plausible GUT model. Among them we considered the gauge coupling unification, the proton stability constraints, the smallness of the active neutrino masses, and nontrivial LHC phenomenology. Towards this end, we specified the simplest benchmark models of the non-SM particle spectrum lighter than the GUT scale and which meet these conditions. We examined two of them and found that they may give rise to observable signals at the LHC, as well as contain a viable scalar CDM particle candidate. In order to account for the observed DM relic abundance in the Universe, the latter imposes certain constraints on the model parameter space. From this DM condition we found, in particular, the lower limits in the mass of the seesaw type-III mediator (m_S), for the two simple benchmark models analyzed in the paper. It is worth noting that *Model (1)* is manifestly falsifiable, as seen from Fig. 1. A relatively small improvement of the proton decay lifetime lower limit up to $\sim 6 \times 10^{15}$ GeV would reject the model.

Various aspects of the adjoint $SU(5)$ scenario have been studied in the literature [41,43,100]. In Refs. [41,43], the fact that ρ_3 is the lightest field in the **24** offers a viable way to understand the baryogenesis via leptogenesis. In this work, we also considered the field ρ_3 as the lightest component of the **24**, and therefore the baryogenesis can be accomplished in our model in the same way. Note also that in this mechanism [100], the decays of the ρ_3 create a lepton asymmetry, which then is converted in a baryon asymmetry by the sphalerons. Imposing the condition of the successful leptogenesis and for the normal hierarchy of neutrinos, one finds that the mass of ρ_3 should be large, which is in agreement with the large ρ_3 mass values predicted in the present paper.

Finally, as was previously noticed in Ref. [43], the mass of ρ_8 must be heavier than 10^6 GeV–10^7 GeV in order to satisfy the constraints from the big bang nucleosynthesis for the GUT scales larger than 3×10^{15} GeV. This condition is also consistent with our results, where the mass of this field is set around the GUT scale.

ACKNOWLEDGMENTS

We are grateful to Martin Hirsch for valuable discussions and recommendations. We also thank Ernest Ma and Ivan Girardi for useful comments. This work was partially supported by Fondecyt (Chile), Grants No. 11130115, No. 1150792, No. 1140390, No. 3150472, and by DGIP internal Grant No. 111458.

APPENDIX A: THE PRODUCT RULES FOR T_7

The group T_7 is the minimal non-Abelian discrete group having a complex triplet. The discrete group T_7 has 21 elements and 5 irreps—i.e., one triplet **3**, one antitriplet $\overline{\mathbf{3}}$, and three singlets $\mathbf{1}_0$, $\mathbf{1}_1$ and $\mathbf{1}_2$ [12]. Furthermore, the T_7 group is a subgroup of $SU(3)$ and $\Delta(3N^2)$ with $N = 7$ and is isomorphic to $Z_7 \rtimes Z_3$. The triplet and antitriplet irreducible representations can be defined as follows [12]:

$$\mathbf{3} \equiv \begin{pmatrix} x_1 \\ x_2 \\ x_4 \end{pmatrix}, \qquad \overline{\mathbf{3}} \equiv \begin{pmatrix} x_{-1} \\ x_{-2} \\ x_{-4} \end{pmatrix} = \begin{pmatrix} x_6 \\ x_5 \\ x_3 \end{pmatrix}. \quad \text{(A1)}$$

The triplet and antitriplet T_7 tensor irreducible representations satisfy the following product rules:

$$\begin{aligned} &\begin{pmatrix} x_1 \\ x_2 \\ x_4 \end{pmatrix}_{\mathbf{3}} \otimes \begin{pmatrix} y_1 \\ y_2 \\ y_4 \end{pmatrix}_{\mathbf{3}} \\ &= \begin{pmatrix} x_2 y_4 \\ x_4 y_1 \\ x_1 y_2 \end{pmatrix}_{\overline{\mathbf{3}}} \oplus \begin{pmatrix} x_4 y_2 \\ x_1 y_4 \\ x_2 y_1 \end{pmatrix}_{\overline{\mathbf{3}}} \oplus \begin{pmatrix} x_4 y_4 \\ x_1 y_1 \\ x_2 y_2 \end{pmatrix}_{\mathbf{3}}, \end{aligned} \quad \text{(A2)}$$

$$\begin{pmatrix} x_6 \\ x_5 \\ x_3 \end{pmatrix}_{\bar{\mathbf{3}}} \otimes \begin{pmatrix} y_6 \\ y_5 \\ y_3 \end{pmatrix}_{\bar{\mathbf{3}}} = \begin{pmatrix} x_5 y_3 \\ x_3 y_6 \\ x_6 y_5 \end{pmatrix}_{\mathbf{3}} \oplus \begin{pmatrix} x_3 y_5 \\ x_6 y_3 \\ x_5 y_6 \end{pmatrix}_{\mathbf{3}} \oplus \begin{pmatrix} x_3 y_3 \\ x_6 y_6 \\ x_5 y_5 \end{pmatrix}_{\bar{\mathbf{3}}}, \tag{A3}$$

$$\begin{pmatrix} x_1 \\ x_2 \\ x_4 \end{pmatrix}_{\mathbf{3}} \otimes \begin{pmatrix} y_6 \\ y_5 \\ y_3 \end{pmatrix}_{\bar{\mathbf{3}}} = \begin{pmatrix} x_2 y_6 \\ x_4 y_5 \\ x_1 y_3 \end{pmatrix}_{\mathbf{3}} \oplus \begin{pmatrix} x_1 y_5 \\ x_2 y_3 \\ x_4 y_6 \end{pmatrix}_{\bar{\mathbf{3}}} \oplus \sum_{k=0,1,2} (x_1 y_6 + \omega^k x_2 y_5 + \omega^{2k} x_4 y_3)_{\mathbf{1}_k}. \tag{A4}$$

Whereas the tensor products between singlets are given by the relations

$$\begin{aligned} &(x)_{\mathbf{1}_0}(y)_{\mathbf{1}_0} = (x)_{\mathbf{1}_1}(y)_{\mathbf{1}_2} = (x)_{\mathbf{1}_2}(y)_{\mathbf{1}_1} = (xy)_{\mathbf{1}_0}, \\ &(x)_{\mathbf{1}_1}(y)_{\mathbf{1}_1} = (xy)_{\mathbf{1}_2}, \\ &(x)_{\mathbf{1}_2}(y)_{\mathbf{1}_2} = (xy)_{\mathbf{1}_1}, \end{aligned} \tag{A5}$$

the product rules between triplets and singlets read

$$(y)_{\mathbf{1}_k} \otimes \begin{pmatrix} x_{1(6)} \\ x_{2(5)} \\ x_{4(3)} \end{pmatrix}_{\mathbf{3}(\bar{\mathbf{3}})} = \begin{pmatrix} y x_{1(6)} \\ y x_{2(5)} \\ y x_{4(3)} \end{pmatrix}_{\mathbf{3}(\bar{\mathbf{3}})}. \tag{A6}$$

where $\omega = e^{i\frac{2\pi}{3}}$. The representation $\mathbf{1}_0$ is trivial, while the nontrivial $\mathbf{1}_1$ and $\mathbf{1}_2$ are complex conjugate to each other. Some reviews of discrete symmetries in particle physics can be found in Refs. [11,12,39,101].

APPENDIX B: ON THE UNIVERSALITY OF YUKAWA COUPLINGS

The aforementioned scheme of approximate universality of dimensionless couplings can be justified by adding an extra Z_{24} symmetry and four $SU(5)$ scalar singlets, assigned as T_7 trivial singlets, as well as by setting their VEVs to be equal to $\lambda\Lambda$, with $\lambda = 0.225$, one of the Wolfenstein parameters, and Λ being our model cutoff. One of the four $SU(5)$ scalar singlets, namely S, can be assumed to have the same Z_{12} charge as the scalar field σ of our model and can also be made charged under the new Z_{24} symmetry and neutral under the remaining cyclic symmetries. The remaining three $SU(5)$ scalar singlets, namely Δ_i $(i = 1, 2, 3)$, can be assumed to be only charged under the new Z_{24} symmetry. These four new scalar fields will transform under the Z_{24} symmetry as follows:

$$\begin{aligned} &S \to e^{-i\frac{\pi}{6}} S, \qquad \Delta_1 \to i\Delta_1, \\ &\Delta_2 \to e^{i\frac{\pi}{3}} \Delta_2, \qquad \Delta_3 \to e^{i\frac{\pi}{4}} \Delta_3. \end{aligned} \tag{B1}$$

The aforementioned Z_{24} charge assignments will generate the following Z_{24} neutral combinations of the new scalar fields:

$$S^6\Delta_1^2, \qquad S^4\Delta_2^2, \qquad S^3\Delta_3^2. \tag{B2}$$

These Z_{24} neutral combinations will give rise to the following Yukawa operators invariant under the symmetries of the model:

$$\begin{aligned} &\varepsilon^{ijklp} \Psi^{(1)}_{ij} H^{(2)}_p \Psi^{(1)}_{kl} \frac{S^6\Delta_1^2}{\Lambda^8}, \\ &\varepsilon^{ijklp} \Psi^{(2)}_{ij} H^{(3)}_p \Psi^{(2)}_{kl} \frac{S^4\Delta_2^2}{\Lambda^6}, \\ &\varepsilon^{ijklp} \Psi^{(1)}_{ij} H^{(3)}_p \Psi^{(3)}_{kl} \frac{S^3\Delta_3^2}{\Lambda^5}, \\ &\varepsilon^{ijklp} \Psi^{(3)}_{ij} H^{(3)}_p \Psi^{(1)}_{kl} \frac{S^3\Delta_3^2}{\Lambda^5}. \end{aligned} \tag{B3}$$

The first two aforementioned Yukawa operators will contribute to the 11 and 22 entries of the up-type quark mass matrix, whereas the last two operators will contribute to the 13 and 31 entries. These new contributions will be proportional to λ^8, λ^6, and λ^5, respectively, and thus will introduce deviations from the exact universality in the dimensionless Yukawa couplings. These aforementioned contributions will correspond to the first-order term in the λ expansion of the expressions given in Eq. (41).

APPENDIX C: SIMPLE BENCHMARK MODELS

The contributions to the $\Delta b'$ coefficients for each field in the 5_s, 24_s, 45_s, and 24_f reps are shown in Table IV. In Table V, the configurations which generate neutrino mass in agreement with the mechanism described in Sec. III are shown. Each particle content, added to the SM, lead to "SM + X" configurations unifying gauge couplings almost equal to or better than the MSSM—i.e, each one of the simplest configurations satisfies $\alpha_2^{-1}(m_G) - \alpha_1^{-1}(m_G) \lesssim \alpha_{2\mathrm{MSSM}}^{-1}(m_G) - \alpha_{1\mathrm{MSSM}}^{-1}(m_G)$ and 3×10^{15} GeV$\lesssim m_G \lesssim 10^{18}$ GeV in order to obtain proton lifetimes allowed by the actual experimental bounds.

TABLE IV. Contribution to the running of the gauge couplings of the fields from the 5_s, 24_s, 45_s, and 24_f representations of the $SU(5)$. The seesaw particle mediators N_R and $\rho_{0,3}$ are added at 10^{14} GeV, contributing to the running of the gauge couplings with $(0, 4/3, 0)$ in the range $[10^{14}\ \text{GeV}, m_G]$. The contribution of the fields in the 24_f is twice the contribution of 24_s owing to its fermionic nature.

$SU(5)$ rep	Fields	$\Delta b'_{1,2,3}$
5_S	H_1, H_2	$(\frac{1}{10}, \frac{1}{6}, 0)$, $(\frac{1}{15}, 0, \frac{1}{6})$
24_S	Ξ_1, Ξ_3, Ξ_8, $\Xi_{(3,2)}$, $\Xi_{(\bar{3},2)}$	$(0, 0, 0)$, $(0, \frac{2}{3}, 0)$, $(0, 0, 1)$, $(\frac{5}{6}, \frac{1}{2}, \frac{1}{3})$, $(\frac{5}{6}, \frac{1}{2}, \frac{1}{3})$
45_S	Φ_1, Φ_2, Φ_3, Φ_4, Φ_5, Φ_6, Φ_7	$(\frac{1}{10}, \frac{1}{6}, 0)$, $(\frac{1}{15}, 0, \frac{1}{6})$, $(\frac{1}{5}, 2, \frac{1}{2})$ $(\frac{4}{15}, 0, \frac{1}{6})$, $(\frac{1}{30}, \frac{1}{2}, \frac{1}{3})$ $(\frac{2}{15}, 0, \frac{5}{6})$ $(\frac{4}{5}, \frac{4}{3}, 2)$
24_f	ρ_1, ρ_3, ρ_8, $\rho_{(3,2)}$, $\rho_{(\bar{3},2)}$	$(0, 0, 0)$, $(0, \frac{4}{3}, 0)$, $(0, 0, 2)$, $(\frac{5}{3}, 1, \frac{2}{3})$, $(\frac{5}{3}, 1, \frac{2}{3})$

TABLE V. Simple X configurations, leading to the GCU and generating the neutrino mass via type-I and type-III seesaw mechanisms. The masses of all the extra scalar particles Φ_i and Ξ_i are about $m_{\text{NP}} = 2 \times 10^3$ GeV, while the fermionic seesaw mediators N_R, $\rho_{0,3}$ are much heavier, with the masses at the scale $m_S = 10^{14}$ GeV. The $\Delta b'$ RGE coefficients correspond to the contribution of the scalars. The seesaw mediators contribute with an extra $(0, 4/3, 0)$ above the scale 10^{14} GeV.

(X)	Model (X)	$\Delta b'_{1,2,3}$	m_G	$SU(5)$ Reps
(1)	$\Xi_8 + 2\Xi_3 + N_R + \rho_0 + \rho_3$	$(0, \frac{4}{3}, 1)$	2.82×10^{15}	$1 + 24_s + 24_f$
(2)	$2\Phi_7 + \Phi_1 + \Xi_3 + N_R + \rho_0 + \rho_3$	$(\frac{17}{10}, \frac{7}{2}, 4)$	4.17×10^{17}	$1 + 24_s + 45_s + 24_f$
(3)	$2\Phi_7 + 2\Phi_1 + \Xi_3 + N_R + \rho_0 + \rho_3$	$(\frac{9}{5}, \frac{11}{3}, 4)$	1.34×10^{17}	$1 + 24_s + 45_s + 24_f$
(4)	$2\Xi_3 + \Phi_6 + \Phi_7 + N_R + \rho_0 + \rho_3$	$(\frac{14}{15}, \frac{8}{3}, \frac{17}{6})$	4.74×10^{16}	$1 + 24_s + 45_s + 24_f$
(5)	$3\Xi_3 + 2\Xi_8 + \Xi_{(3,2)} + N_R + \rho_0 + \rho_3$	$(\frac{5}{6}, \frac{5}{2}, \frac{7}{3})$	6.8×10^{15}	$1 + 24_s + 45_s + 24_f$
(6)	$\Phi_2 + 2\Xi_3 + \Xi_8 + N_R + \rho_0 + \rho_3$	$(\frac{1}{15}, \frac{4}{3}, \frac{7}{6})$	6.8×10^{15}	$1 + 24_s + 45_s + 24_f$
(7)	$\Phi_2 + 3\Xi_3 + 2\Xi_8 + \Xi_{(3,2)} + N_R + \rho_0 + \rho_3$	$(\frac{9}{10}, \frac{5}{2}, \frac{5}{2})$	1.7×10^{16}	$1 + 24_s + 45_s + 24_f$
(8)	$2\Phi_6 + \Phi_3 + N_R + \rho_0 + \rho_3$	$(\frac{7}{15}, 2, \frac{13}{6})$	4.6×10^{16}	$1 + 45_s + 24_f$
(9)	$\Phi_2 + 2\Phi_7 + \Phi_3 + \Phi_4 + N_R + \rho_0 + \rho_3$	$(\frac{44}{15}, \frac{14}{3}, \frac{29}{6})$	4.63×10^{16}	$1 + 45_s + 24_f$
(10)	$2\Phi_7 + \Phi_3 + \Phi_4 + \Xi_{(3,2)} + N_R + \rho_0 + \rho_3$	$(\frac{37}{10}, \frac{31}{6}, 5)$	6.77×10^{15}	$1 + 24_s + 45_s + 24_f$
(11)	$3\Phi_7 + \Phi_3 + \Phi_4 + \Xi_{(3,2)} + N_R + \rho_0 + \rho_3$	$(\frac{9}{2}, \frac{13}{2}, 7)$	4.17×10^{17}	$1 + 24_s + 45_s + 24_f$
(12)	$\Phi_6 + 2\Phi_7 + \Phi_3 + 3\Xi_{(3,2)} + N_R + \rho_0 + \rho_3$	$(\frac{133}{30}, \frac{37}{6}, \frac{19}{3})$	4.63×10^{16}	$1 + 24_s + 45_s + 24_f$

[1] G. Aad *et al.* (ATLAS Collaboration), Phys. Lett. B **716**, 1 (2012); S. Chatrchyan *et al.* (CMS Collaboration), Phys. Lett. B **716**, 30 (2012).

[2] J. Beringer *et al.* (Particle Data Group), Phys. Rev. D **86**, 010001 (2012).

[3] F. P. An *et al.* (DAYA-BAY Collaboration), Phys. Rev. Lett. **108**, 171803 (2012).

[4] K. Abe *et al.* (T2K Collaboration), Phys. Rev. Lett. **107**, 041801 (2011).

[5] P. Adamson *et al.* (MINOS Collaboration), Phys. Rev. Lett. **107**, 181802 (2011).

[6] Y. Abe *et al.* (DOUBLE-CHOOZ Collaboration), Phys. Rev. Lett. **108**, 131801 (2012).

[7] J. K. Ahn *et al.* (RENO Collaboration), Phys. Rev. Lett. **108**, 191802 (2012).

[8] D. V. Forero, M. Tortola, and J. W. F. Valle, Phys. Rev. D **90**, 093006 (2014).

[9] H. Fritzsch and Z.-z. Xing, Prog. Part. Nucl. Phys. **45**, 1 (2000).

[10] G. Altarelli and F. Feruglio, Springer Tracts Mod. Phys. **190**, 169 (2003).

[11] G. Altarelli and F. Feruglio, Rev. Mod. Phys. **82**, 2701 (2010).

[12] H. Ishimori, T. Kobayashi, H. Ohki, Y. Shimizu, H. Okada, and M. Tanimoto, Prog. Theor. Phys. Suppl. **183**, 1 (2010).

[13] S. F. King, A. Merle, S. Morisi, Y. Shimizu, and M. Tanimoto, New J. Phys. **16**, 045018 (2014).

[14] M. Gupta and G. Ahuja, Int. J. Mod. Phys. A **27**, 1230033 (2012); H. Pas and E. Schumacher, Phys. Rev. D **89**, 096010 (2014); A. E. C. Hernández, E. C. Mur, and R. Martinez, Phys. Rev. D **90**, 073001 (2014); A. E. C. Hernández and I. de Medeiros Varzielas, J. Phys. G **42**, 065002 (2015); H. Nishiura and T. Fukuyama, Mod. Phys. Lett. A **29**, 1450147 (2014); M. Frank, C. Hamzaoui, N. Pourtolami, and M. Toharia, Phys. Lett. B **742**, 178 (2015); R. Sinha, R. Samanta, and A. Ghosal, arXiv:1508.05227; H. Nishiura and T. Fukuyama, arXiv:1510.01035; R. R. Gautam, M. Singh, and M. Gupta, Phys. Rev. D **92**, 013006 (2015); H. Pas and E. Schumacher, arXiv:1510.08757.

[15] D. Marzocca, S. T. Petcov, A. Romanino, and M. Spinrath, J. High Energy Phys. 11 (2011) 009.

[16] S. Antusch, C. Gross, V. Maurer, and C. Sluka, Nucl. Phys. **B877**, 772 (2013).

[17] S. Fichet, B. Herrmann, and Y. Stoll, Phys. Lett. B **742**, 69 (2015).

[18] M.-C. Chen, J. Huang, K. T. Mahanthappa, and A. M. Wijangco, J. High Energy Phys. 10 (2013) 112.

[19] S. F. King, C. Luhn, and A. J. Stuart, Nucl. Phys. **B867**, 203 (2013).

[20] D. Meloni, J. High Energy Phys. 10 (2011) 010.

[21] P. S. Bhupal Dev, B. Dutta, R. N. Mohapatra, and M. Severson, Phys. Rev. D **86**, 035002 (2012).

[22] K. S. Babu and Y. Meng, Phys. Rev. D **80**, 075003 (2009).

[23] K. S. Babu, K. Kawashima, and J. Kubo, Phys. Rev. D **83**, 095008 (2011).

[24] J. C. Gómez-Izquierdo, F. González Canales, and M. Mondragón, Eur. Phys. J. C **75**, 221 (2015).

[25] S. Antusch, S. F. King, and M. Spinrath, Phys. Rev. D **83**, 013005 (2011).

[26] C. Hagedorn, S. F. King, and C. Luhn, J. High Energy Phys. 06 (2010) 048.

[27] H. Ishimori, Y. Shimizu, and M. Tanimoto, Prog. Theor. Phys. **121**, 769 (2009).

[28] K. M. Patel, Phys. Lett. B **695**, 225 (2011).

[29] I. K. Cooper, S. F. King, and C. Luhn, Phys. Lett. B **690**, 396 (2010).

[30] D. Emmanuel-Costa, C. Simoes, and M. Tortola, J. High Energy Phys. 10 (2013) 054.

[31] M.-C. Chen and K. T. Mahanthappa, Phys. Lett. B **652**, 34 (2007).

[32] S. Antusch, I. de Medeiros Varzielas, V. Maurer, C. Sluka, and M. Spinrath, J. High Energy Phys. 09 (2014) 141.

[33] J. Gehrlein, J. P. Oppermann, D. Schafer, and M. Spinrath, Nucl. Phys. **B890**, 539 (2014).

[34] M. D. Campos, A. E. C. Hernández, S. Kovalenko, I. Schmidt, and E. Schumacher, Phys. Rev. D **90**, 016006 (2014).

[35] A. E. C. Hernández, S. G. Kovalenko, and I. Schmidt, arXiv:1411.2913.

[36] J. Gehrlein, S. T. Petcov, M. Spinrath, and X. Zhang, Nucl. Phys. **B896**, 311 (2015).

[37] F. Bjorkeroth, F. J. de Anda, I. de Medeiros Varzielas, and S. F. King, J. High Energy Phys. 06 (2015) 141.

[38] M.-C. Chen and K. T. Mahanthappa, Int. J. Mod. Phys. A **18**, 5819 (2003).

[39] S. F. King and C. Luhn, Rep. Prog. Phys. **76**, 056201 (2013).

[40] C. Luhn, S. Nasri, and P. Ramond, Phys. Lett. B **652**, 27 (2007); C. Hagedorn, M. A. Schmidt, and A. Y. Smirnov, Phys. Rev. D **79**, 036002 (2009); Q. H. Cao, S. Khalil, E. Ma, and H. Okada, Phys. Rev. Lett. **106**, 131801 (2011); C. Luhn, K. M. Parattu, and A. Wingerter, J. High Energy Phys. 12 (2012) 096 (2012); J. Kile, M. J. Pérez, P. Ramond, and J. Zhang, J. High Energy Phys. 02 (2014) 036; 11 (2014) 158; Y. Kajiyama, H. Okada, and K. Yagyu, J. High Energy Phys. 10 (2013) 196; V. V. Vien and H. N. Long, J. High Energy Phys. 04 (2014) 133; C. Bonilla, S. Morisi, E. Peinado, and J. W. F. Valle, Phys. Lett. B **742**, 99 (2015); J. Kile, M. J. Pérez, P. Ramond, and J. Zhang, Phys. Rev. D **90**, 013004 (2014); A. E. C. Hernández and R. Martinez, arXiv:1501.07261.

[41] P. F. Perez, Phys. Lett. B **654**, 189 (2007).

[42] P. F. Pèrez, in *Proceedings of the 15th International Conference on Supersymmetry and the Unification of Fundamental Interactions, Karlsruhe, Germany, 2007*, edited by W. de Boer and I. Gebauer, pp. 678–681.

[43] P. F. Pèrez, H. Iminniyaz, and Germán Rodrigo, Phys. Rev. D **78**, 015013 (2008).

[44] H. Georgi and S. L. Glashow, Phys. Rev. Lett. **32**, 438 (1974).

[45] H. Georgi and C. Jarlskog, Phys. Lett. **86B**, 297 (1979).

[46] P. Frampton, S. Nandi, and J. Scanio, Phys. Lett. **85B**, 225 (1979).

[47] J. R. Ellis and M. K. Gaillard, Phys. Lett. **88B**, 315 (1979).

[48] S. Nandi and K. Tanaka, Phys. Lett. **92B**, 107 (1980).

[49] P. H. Frampton, Phys. Lett. **89B**, 352 (1980).

[50] P. Langacker, Phys. Rep. **72**, 185 (1981).

[51] P. Kalyniak and J. N. Ng, Phys. Rev. D **26**, 890 (1982).

[52] A. Giveon, L. J. Hall, and U. Sarid, Phys. Lett. B **271**, 138 (1991).

[53] I. Dorsner and I. Mocioiu, Nucl. Phys. **B796**, 123 (2008).

[54] S. Khalil and S. Salem, Nucl. Phys. **B876**, 473 (2013).

[55] I. Dorsner and P. F. Perez, Phys. Lett. B **642**, 248 (2006).

[56] L.-F. Li, Phys. Rev. D **9**, 1723 (1974).

[57] W. Grimus and L. Lavoura, J. High Energy Phys. 11 (2000) 042.

[58] C. Alvarado, R. Martinez, and F. Ochoa, Phys. Rev. D **86**, 025027 (2012).

[59] A. E. Carcamo Hernandez, R. Martinez, and F. Ochoa, Phys. Rev. D **87**, 075009 (2013).

[60] A. E. C. Hernández, I. de Medeiros Varzielas, S. G. Kovalenko, H. Päs, and I. Schmidt, Phys. Rev. D **88**, 076014 (2013).

[61] W. Grimus and L. Lavoura, J. High Energy Phys. 09 (2008) 106; Phys. Lett. B **671**, 456 (2009); C. S. Lam, arXiv:0907.2206; C. H. Albright and W. Rodejohann, Eur. Phys. J. C **62**, 599 (2009); C. H. Albright, A. Dueck, and W. Rodejohann, Eur. Phys. J. C **70**, 1099 (2010); S. Antusch, S. F. King, C. Luhn, and M. Spinrath, Nucl. Phys. **B856**, 328 (2012); C. C. Li and G. J. Ding, Nucl. Phys. **B881**, 206 (2014).

[62] M. Auger *et al.* (EXO Collaboration), Phys. Rev. Lett. **109**, 032505 (2012).
[63] I. Abt *et al.* (GERDA Collaboration), arXiv:hep-ex/0404039.
[64] K.-H. Ackermann *et al.* (GERDA Collaboration), Eur. Phys. J. C **73**, 2330 (2013).
[65] F. Alessandria *et al.*, arXiv:1109.0494.
[66] A. Gando *et al.* (KamLAND-Zen Collaboration), Phys. Rev. C **85**, 045504 (2012).
[67] D. Auty (EXO-200 Collaboration), Recontres de Moriond, http://moriond.in2p3.fr/.
[68] C. Aalseth *et al.* (Majorana Collaboration), Nucl. Phys. B, Proc. Suppl. **217**, 44 (2011).
[69] O. Cremonesi and M. Pavan, Adv. High Energy Phys. **2014**, 1 (2014); W. Rodejohann, J. Phys. G **39**, 124008 (2012); A. Barabash, arXiv:1209.4241; F. F. Deppisch, M. Hirsch, and H. Päs, J. Phys. G **39**, 124007 (2012); J. Vergados, H. Ejiri, and F. Simkovic, Rep. Prog. Phys. **75**, 106301 (2012); A. Giuliani and A. Poves, Adv. High Energy Phys. **2012**, 1 (2012); S. M. Bilenky and C. Giunti, Int. J. Mod. Phys. A **30**, 1530001 (2015).
[70] K. Bora, arXiv:1206.5909.
[71] Z. z. Xing, H. Zhang, and S. Zhou, Phys. Rev. D **77**, 113016 (2008).
[72] G. C. Branco, D. Emmanuel-Costa, and C. Simoes, Phys. Lett. B **690**, 62 (2010).
[73] A. E. C. Hernández and R. Rahman, arXiv:1007.0447.
[74] A. E. C. Hernández, R. Martinez, and F. Ochoa, arXiv:1309.6567.
[75] S. F. King, S. Morisi, E. Peinado, and J. W. F. Valle, Phys. Lett. B **724**, 68 (2013).
[76] A. E. C. Hernández, R. Martinez, and J. Nisperuza, Eur. Phys. J. C **75**, 72 (2015).
[77] M. D. Campos, A. E. C. Hernández, H. Pas, and E. Schumacher, Phys. Rev. D **91**, 116011 (2015).
[78] A. E. C. Hernández, I. de Medeiros Varzielas, and E. Schumacher, arXiv:1509.02083.
[79] A. E. C. Hernández, N. Neill H, and I. de Medeiros Varzielas, arXiv:1511.07420.
[80] M. Abbas and S. Khalil, Phys. Rev. D **91**, 053003 (2015).
[81] H. Ishimori and S. F. King, Phys. Lett. B **735**, 33 (2014).
[82] Z.-z. Xing, D. Yang, and S. Zhou, Phys. Lett. B **690**, 304 (2010).
[83] G. C. Branco, H. R. C. Ferreira, A. G. Hessler, and J. I. Silva-Marcos, J. High Energy Phys. 05 (2012) 001.
[84] G. Bhattacharyya, I. de Medeiros Varzielas, and P. Leser, Phys. Rev. Lett. **109**, 241603 (2012).
[85] A. E. C. Hernández, C. O. Dib, N. Neill H, and A. R. Zerwekh, J. High Energy Phys. 02 (2012) 132.
[86] V. V. Vien and H. N. Long, J. Korean Phys. Soc. **66**, 1809 (2015).
[87] H. Ishimori, S. F. King, H. Okada, and M. Tanimoto, Phys. Lett. B **743**, 172 (2015).
[88] G. Senjanovic, AIP Conf. Proc. **1200**, 131 (2010).
[89] L. Randall and C. Csaki, in *SUSY 95: International Workshop on Supersymmetry and Unification of Fundamental Interactions, Paliseau, France, 1995*, edited by I. Antoniadis and H. Videau, pp. 99–109.
[90] V. De Romeri, M. Hirsch, and M. Malinsky, Phys. Rev. D **84**, 053012 (2011).
[91] C. Arbelaez, R. M. Fonseca, M. Hirsch, and J. C. Romao, Phys. Rev. D **87**, 075010 (2013).
[92] P. Nath and P. F. Perez, Phys. Rep. **441**, 191 (2007).
[93] K. Abe *et al.* (Super-Kamiokande Collaboration), Phys. Rev. Lett. **113**, 121802 (2014).
[94] C. Biggio and L. Calibbi, J. High Energy Phys. 10 (2010) 037.
[95] G. Aad *et al.* (ATLAS Collaboration), Eur. Phys. J. C **73**, 2263 (2013); **71**, 1828 (2011).
[96] M. Cirelli, N. Fornengo, and A. Strumia, Nucl. Phys. **B753**, 178 (2006); M. Cirelli, A. Strumia, and M. Tamburini, Nucl. Phys. **B787**, 152 (2007).
[97] S. Khalil, S. Salem, and M. Allam, Phys. Rev. D **89**, 095011 (2014).
[98] J. M. Arnold and B. Fornal, Phys. Rev. D **85**, 055020 (2012); S. I. Bityukov and N. V. Krasnikov, Mod. Phys. Lett. A **12**, 2011 (1997); Y. Bai and B. A. Dobrescu, J. High Energy Phys. 07 (2011) 100; M. Gerbush, T. J. Khoo, D. J. Phalen, A. Pierce, and D. Tucker-Smith, Phys. Rev. D **77**, 095003 (2008); X.-G. He, G. Valencia, and H. Yokoya, J. High Energy Phys. 12 (2011) 030; A. Idilbi, C. Kim, and T. Mehen, Phys. Rev. D **82**, 075017 (2010); C. Kim and T. Mehen, Phys. Rev. D **79**, 035011 (2009).
[99] F. Capozzi, G. L. Fogli, E. Lisi, A. Marrone, D. Montanino, and A. Palazzo, Phys. Rev. D **89**, 093018 (2014).
[100] S. Blanchet and P. F. Perez, J. Cosmol. Astropart. Phys. 08 (2008) 037.
[101] P. Ramond, *Group Theory: A Physicist's Survey* (Cambridge University Press, Cambridge, England, 2010); C. Luhn, S. Nasri, and P. Ramond, J. Math. Phys. (N.Y.) **48**, 123519 (2007).